

## Chapter-6

### Variability of NE Monsoon Rainfall

NE monsoon exhibits variability in all time scales, from diurnal, synoptic to intra-seasonal, inter-annual and decadal time scales. In this chapter, the NE Monsoon variability in all time scales is discussed.

#### 6.1. Diurnal Cycle of NE Monsoon Rainfall

The diurnal cycle is one of the most important modes of precipitation variability over the Indian monsoon region (Rajeevan et al. 2012, Bhate et al. 2019, Raj and Amudha 2022). It is a manifestation of the atmosphere-ocean-land-cryosphere response to incoming solar radiation. A detailed analysis and discussions on diurnal variation during the southwest monsoon season are given in Sahany et al. (2010).

This section discusses the results from a detailed analysis of 3-hourly rainfall derived from TRMM satellite data. Harmonic analysis was made to understand the phase and amplitude of diurnal variations. More details of the analysis of diurnal variation are available in Bhate et al. (2019) and Rajeevan et al. (2012).

Fig. 6.1 shows the 3 hourly variation of climatological rainfall over the Indian region during the northeast monsoon season as estimated using TRMM satellite data for the period 1998-2019. It shows distinct types of variations over the Oceans and land. Over the east coast of India, maximum rainfall is observed in the early morning hours, but over the interior parts, rainfall peaks in the late evening and early night.

The spatial map of the phase (hours with maximum rainfall) revealed by the Harmonic Analysis explained is shown in Fig. 6.2. The phase diagram clearly shows the distinct difference in the rainfall peak over the oceans and land. Over the oceans and off the east coast of India, rainfall during the NE monsoon season peaks in the morning. On the other hand, rainfall peaks over the interior parts and the west coast, during the late evening/early night (between 1830 and 2130 IST). Thus, the northeast Monsoon over south peninsular India exhibits significant diurnal variations with large spatial variations.

Along the east coast of India, an early morning peak is observed and over the inland regions and the west coast, an afternoon/evening peaking is observed.

Fig. 6.3 shows hourly average rainfall during the NE monsoon season (Oct-Dec) showing the diurnal variation of observed rainfall over different stations over the south Peninsula. These plots are made using hourly station rainfall data, taken from the IMD archives. These plots clearly suggest that the stations over the east coast experience maximum rainfall during the morning hours. Over the interior parts and the west coast, maximum rainfall occurs during the evening and early night hours. Different physical mechanisms could be responsible for the observed rainfall diurnal variations over land and oceans. The observed rainfall peak in the late afternoon over the land could be due to intense surface solar heating and resultant convective instability. Over the east coast, the presence of a strong sea-land breeze is also noted to be responsible for diurnal variations (Bhate et al., 2019, Ramesh Reddy et al., 2021).

It is important to make a detailed analysis using Numerical Weather Prediction (NWP) model results, whether the NWP models are capable of predicting these observed diurnal variations. An analysis of diurnal variations for the southwest monsoon revealed that NWP model (WRF model) has constraints in predicting diurnal variations accurately (Bhat et al., 2019). The model was found successful in simulating the pattern of diurnal variation of rainfall, but underestimates its amplitude compared to the observed one especially over the western Himalayas, northeast India, central India, and the north Bay of Bengal (BoB). It is important to carry out an extensive analysis to examine how the NWP models are capable of predicting the diurnal variations of NE monsoon rainfall accurately.

## **6.2. Intra-seasonal variation of NE monsoon rainfall**

Several studies have shown that during the southwest monsoon season (June to September) a substantial component of the variability of convection and rainfall over the Indian region arises from the fluctuations on the intra-seasonal scale between active

and weak or break spells (Ramamurthy, 1969; Goswami, 2005; Rajeevan et al., 2010). Long intense breaks are known to have an impact on the seasonal monsoon rainfall over the country (Webster et al., 1998; Gadgil and Joseph, 2003, Rajeevan et al., 2010). The dry and wet spells of the active and break conditions represent the sub-seasonal or intra-seasonal variations of the monsoon with timescales longer than synoptic activity (1–10 days) but shorter than a season.

Recent research results also provided new insights regarding the origin of the monsoon intra-seasonal variations. The ISOs of summer monsoon essentially have timescales between 10 and 90 days. Within the broad range of 10–90 day periods, two period ranges with periodicities between 10 and 20 days and 30 and 60 days respectively are particularly prominent (Goswami, 2005). Active and break spells and intra-seasonal variations of the Indian summer monsoon have been extensively studied. As far as the northeast monsoon is concerned, not much knowledge is available on the intra-seasonal activity during the NE monsoon season. Therefore, the results of the intra-seasonal activity during the northeast monsoon season are discussed in this section.

Fig. 6.4 shows daily rainfall (averaged over the NE monsoon region) from 15 September to 15 January during two sessions, 2008-2009 and 2011-2012. These plots clearly show that rainfall activity over the region is confined to only a few days during the season, which is interspaced between dry or weak monsoon spells. For example, during 2008-2009, heavier rainfall activity was observed around 20-30 October. The next rainfall activity was observed almost after one month, from 20 Nov onwards. Between 30 October to 20 November, rainfall activity over the region was generally subdued. Similar intra-seasonal variability of rainfall with enhanced (suppressed) activity was observed during 2011-12 also.

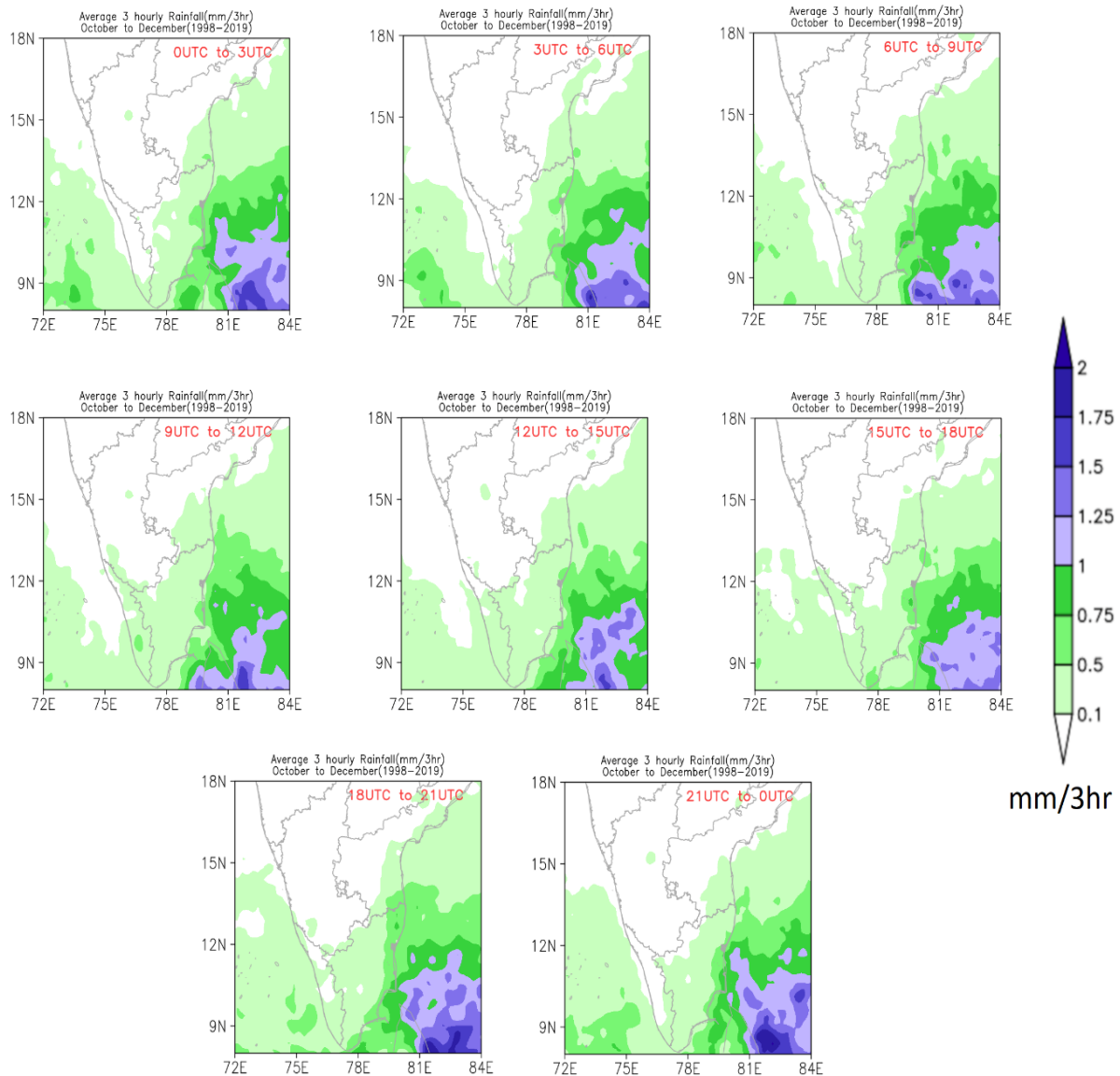


Fig. 6.1. Average 3-hourly seasonal (October to December) rainfall (mm/3hr) over the Indian region averaged over the years 1998-2019 derived from the TRMM 3G68 data.

Fig. 6.5 a shows the Hovmuller diagram showing Outgoing Longwave Radiation (OLR) anomalies averaged over 70<sup>0</sup> -90<sup>0</sup>E plotted with latitude versus time (15 Sept 1998 to 15 January 1999). Fig. 6.5 b shows the similar plot but for the period 15 Sept 2000 to 15 January 2001. OLR is a proxy for atmospheric convection. Low OLR suggests more convection. These two plots clearly show strong intra-seasonal activity during the NE

monsoon season. Fig 6.5 a shows clear northward propagation of OLR anomalies from the equator around 16 October and the next one around 15 November. Another northward propagation is observed around 18 December. However, all the northward propagation of convections are limited to 15°N only. During the southwest monsoon season, this northward propagation moves to even the foothills of the Himalaya. Fig 6.5 b shows a similar plot, but for zonal wind anomalies at 925 hPa. This plot clearly shows the strengthening of the shear zone (between westerlies in the south and easterlies in the north) at particular intervals. This plot also shows the slow southward movement of the horizontal wind shear zone by December, which represents the southward movement of ITCZ.

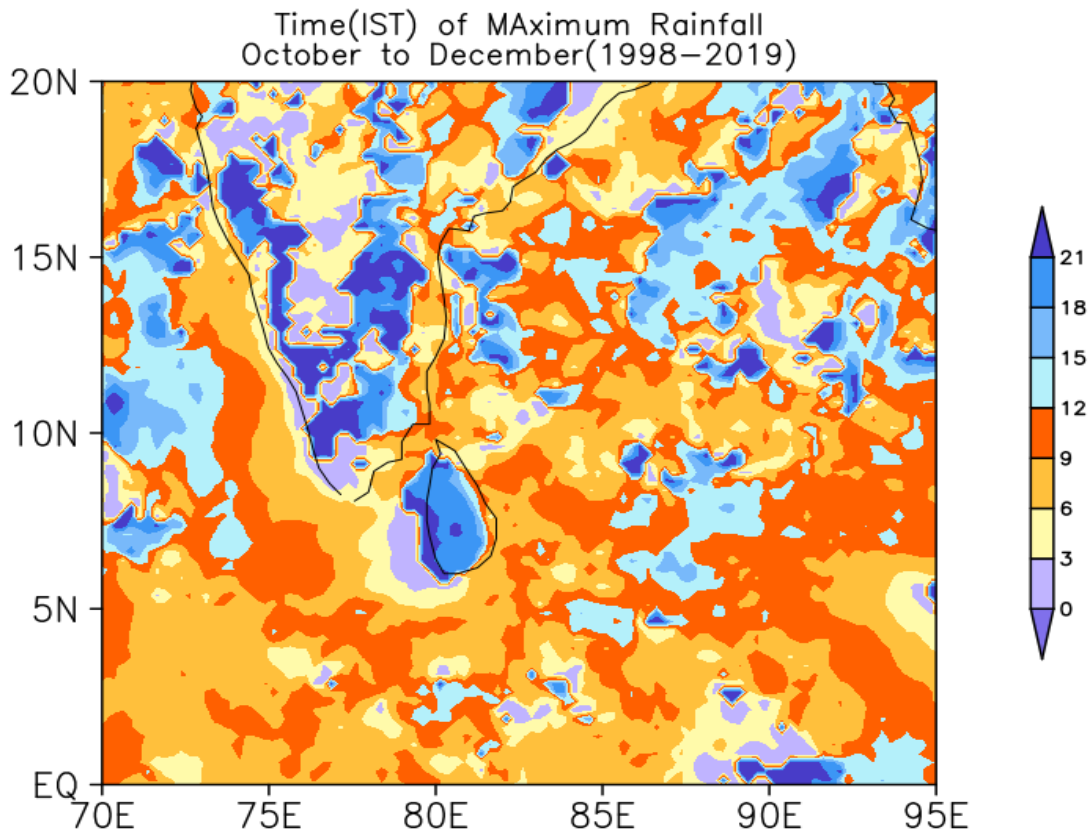
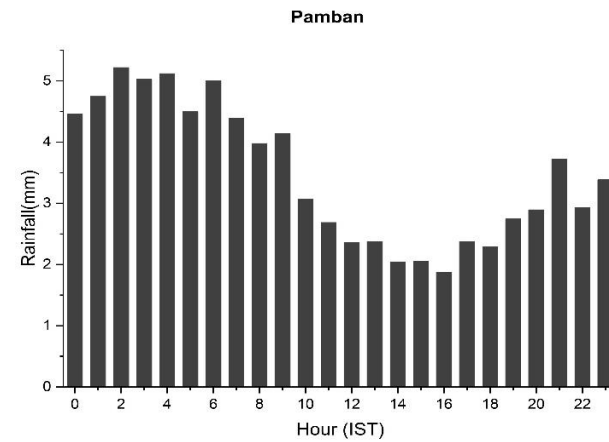
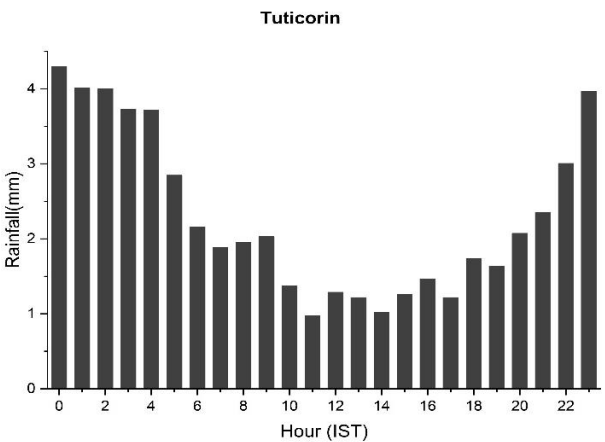
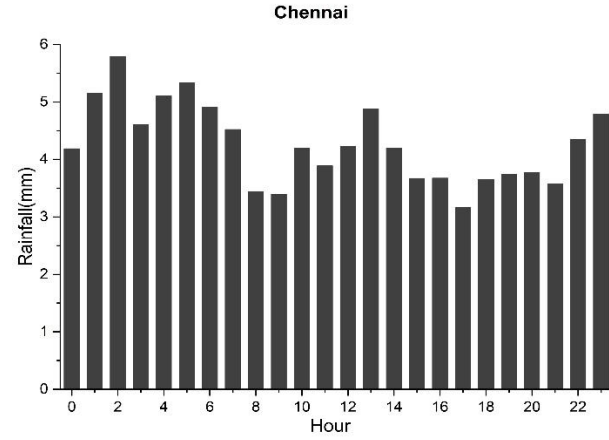
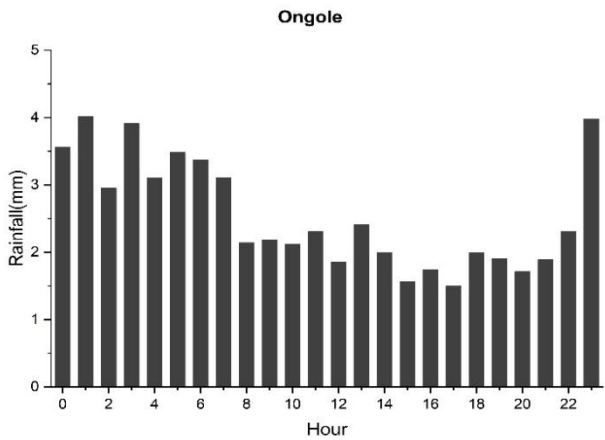
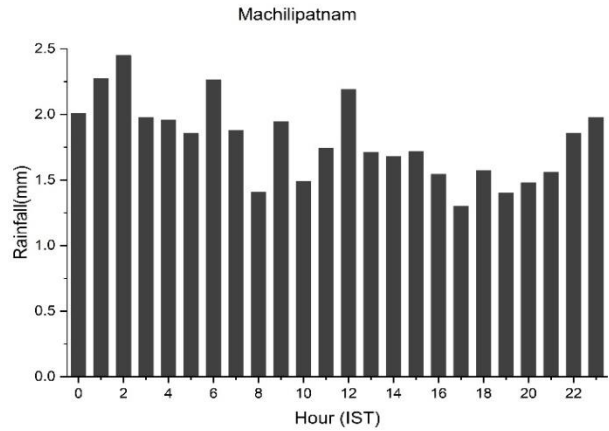
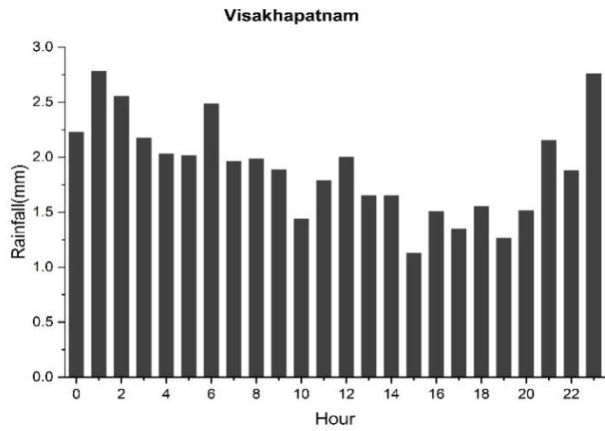
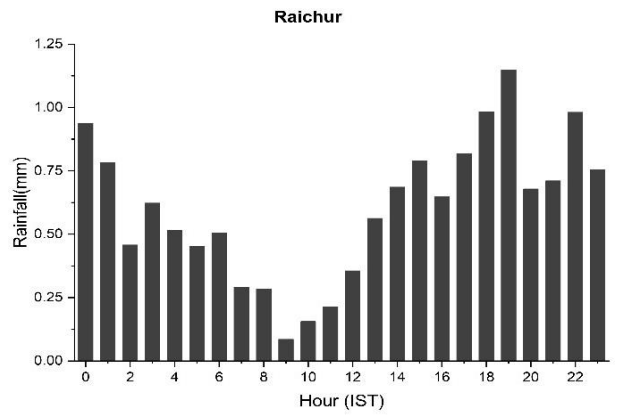
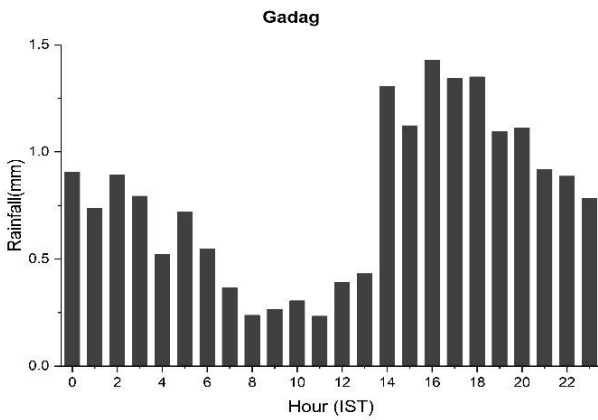
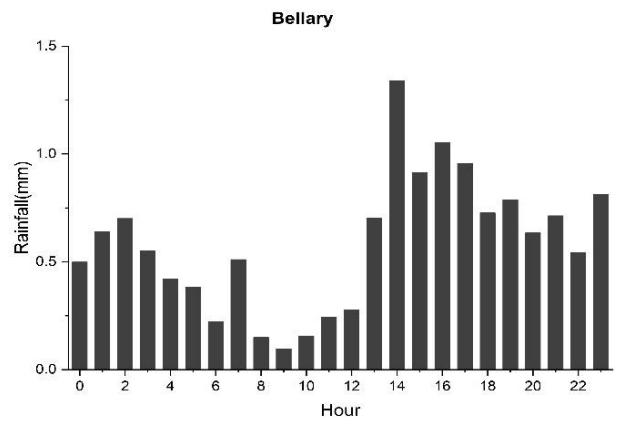
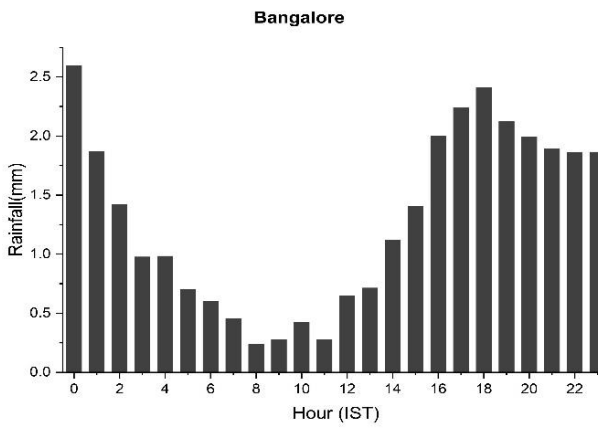
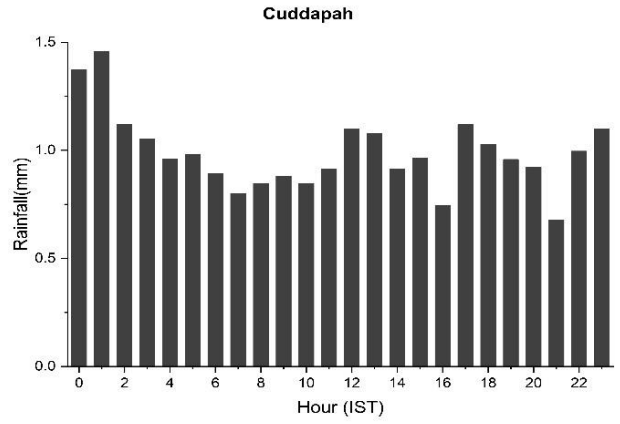
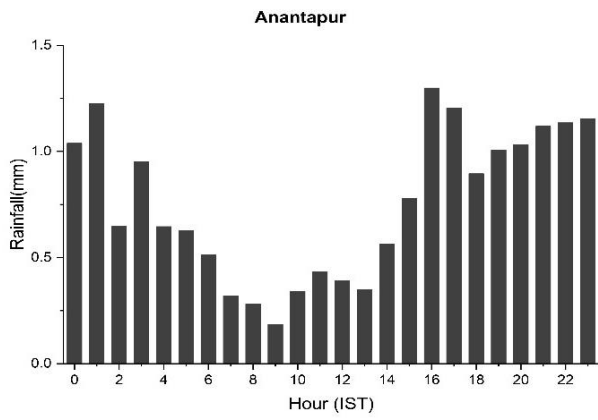


Fig. 6.2. Phase angle (time of maximum rainfall peak) in Indian Standard Time (IST) based on satellite data for the period using the Harmonic Analysis (1998-2019).

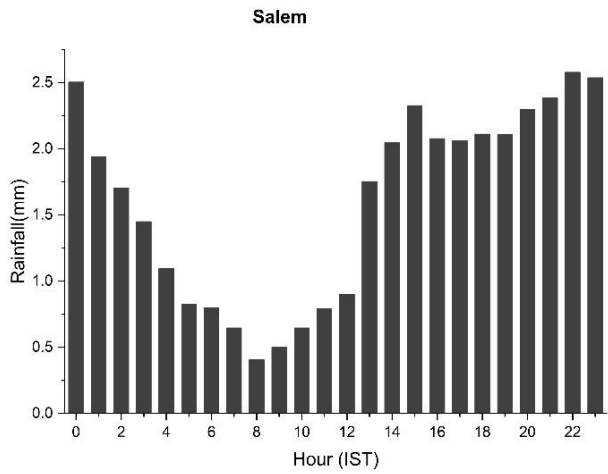
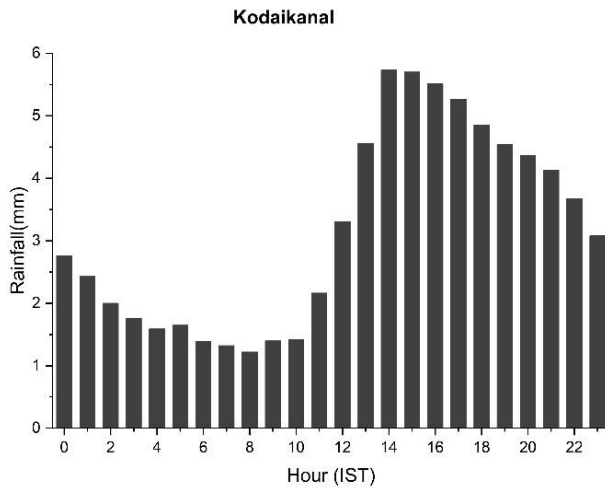
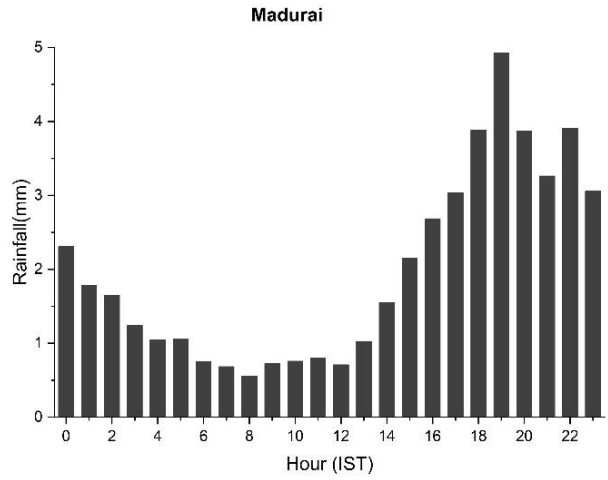
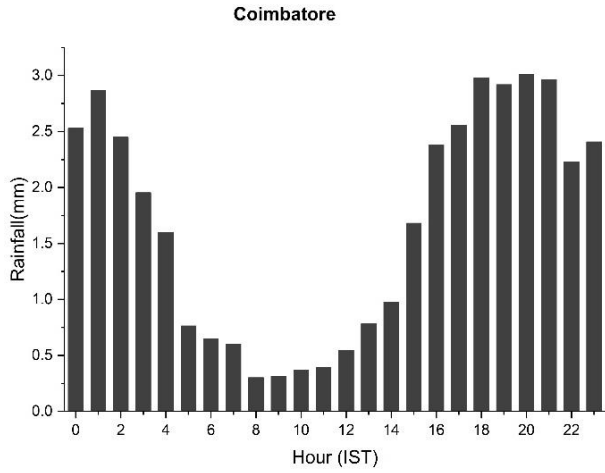
## East Coast stations



## Central Region Stations



## Central Region Stations



## West Coast Stations

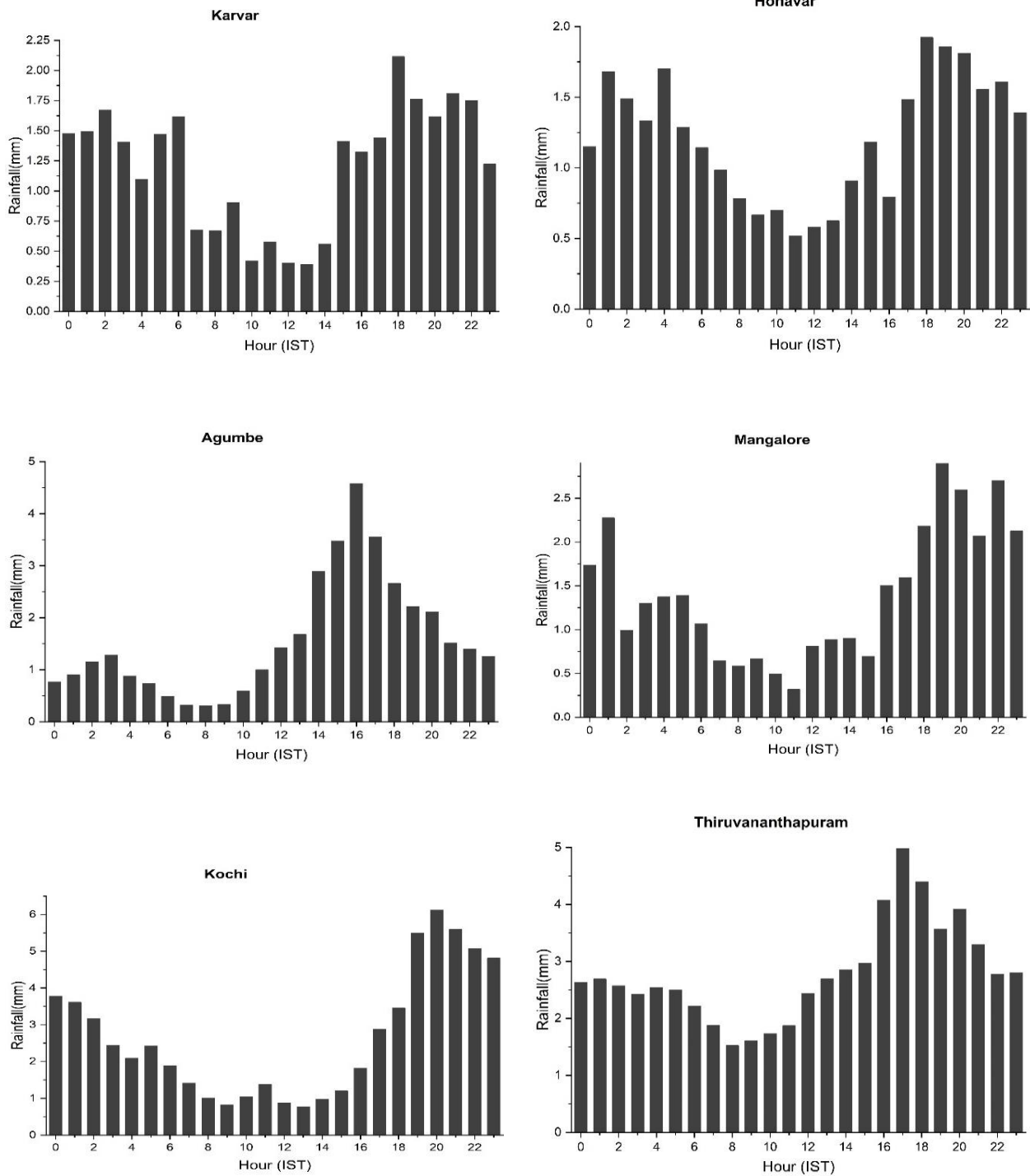


Fig. 6.3. Hourly average rainfall (in mm) during the NE monsoon season (Oct-Dec) showing diurnal variation of rainfall at different stations over south Peninsula. Period: 1969-2021.

Using daily rainfall data from 15 September, 1998 to 15 January 1999, a spectral analysis was made to see the periodicities of rainfall during the NE monsoon season. The results are shown in Fig. 6.6. The spectral analysis shows a strong periodicity of rainfall activity with 30-40 days, which is also statistically significant. Another weaker periodicity is observed around 20 days. Fig 6.6 c shows the wavelet spectrum which also suggests the periodicity around 30-40 days. It may be interesting to note that these two periodicities are predominantly observed during the southwest monsoon season. More studies are required to understand the physical mechanisms of these oscillations during the NE monsoon season. What are the physical mechanisms for these oscillations and what is the predictability of this oscillation?

Sreekala et al., (2018) analyzed intra-seasonal rainfall activity during the NE monsoon season and the combined effect of Madden Julian Oscillation (MJO), NSO and IOD. The study has revealed that the intra-seasonal variation of daily rainfall over the south peninsula during the NEM season is associated with various phases of the eastward propagating MJO life cycle.

A similar study was made using more years of updated data to understand the ISO activity during the NE monsoon season in terms of different phases of MJO. ERA5 (Hersbach et al., 2020) daily precipitation datasets have been used for analyzing the intra-seasonal variation of NE Monsoon rainfall over the Oceanic region. Total hourly precipitation data are used in this study. In addition, zonal and meridional winds at 850 hPa from ERA5 data and Outgoing Long-wave Radiation (OLR) data (Liebmann and Smith 1996) from NCEP/NCAR during 1979-2021 are also used in the current study.

The Real-time Multivariate MJO indices (RMM1 and RMM2) from <http://www.bom.gov.au/bmrc/clfor/cfstaff/matw/maproom/RMM/> were used for defining the various Phases of MJO (Wheeler and Hendon 2004). MJO indices were calculated as the principal component (PC) time series of the two leading empirical

orthogonal functions (EOFs) of combined daily mean fields for 850 and 200 hPa zonal winds and OLR averaged over the tropics ( $15^{\circ}\text{S}$ – $15^{\circ}\text{N}$ ).

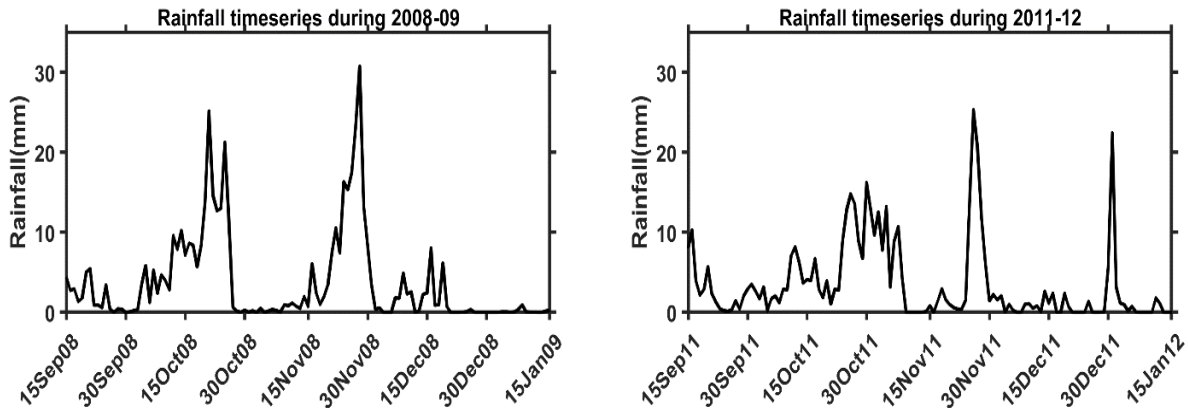


Fig. 6.4. Time series of daily rainfall averaged over NE Monsoon region during 15 September to 15 January a) 2008-2009 b) 2011-2012.

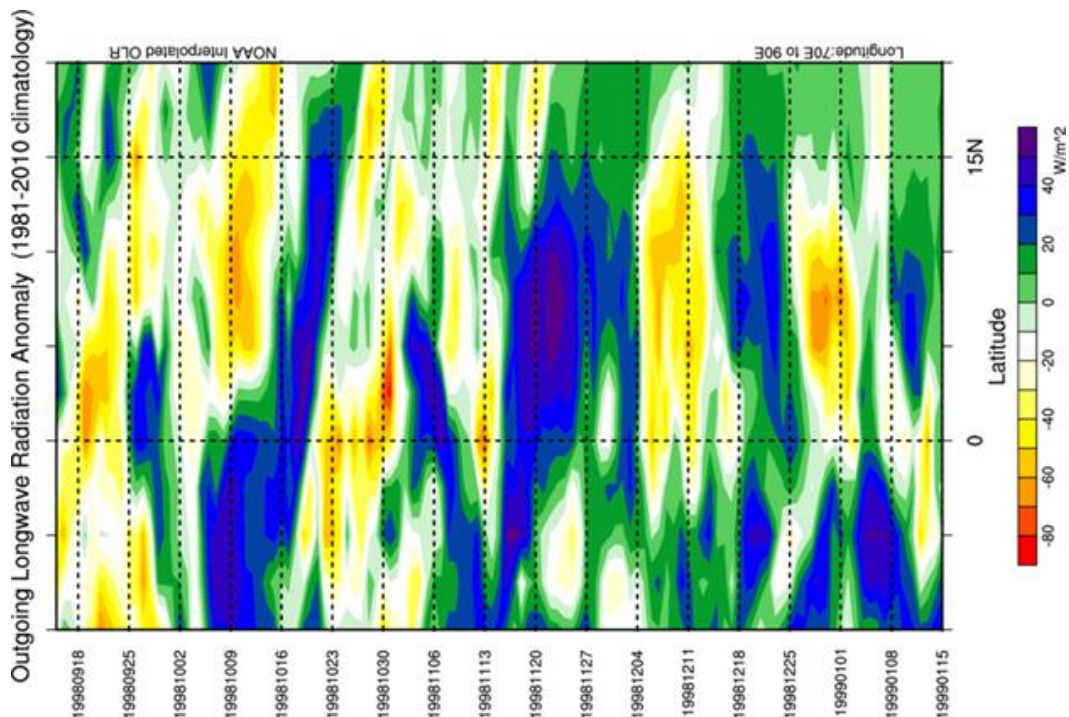


Fig. 6.5 a. Hovmuller diagram (Time vs Latitude) showing northward propagation of convection (OLR anomalies) during 15 September 1998 to 15 January 1999, averaged over  $70^{\circ}$ – $90^{\circ}\text{E}$ .

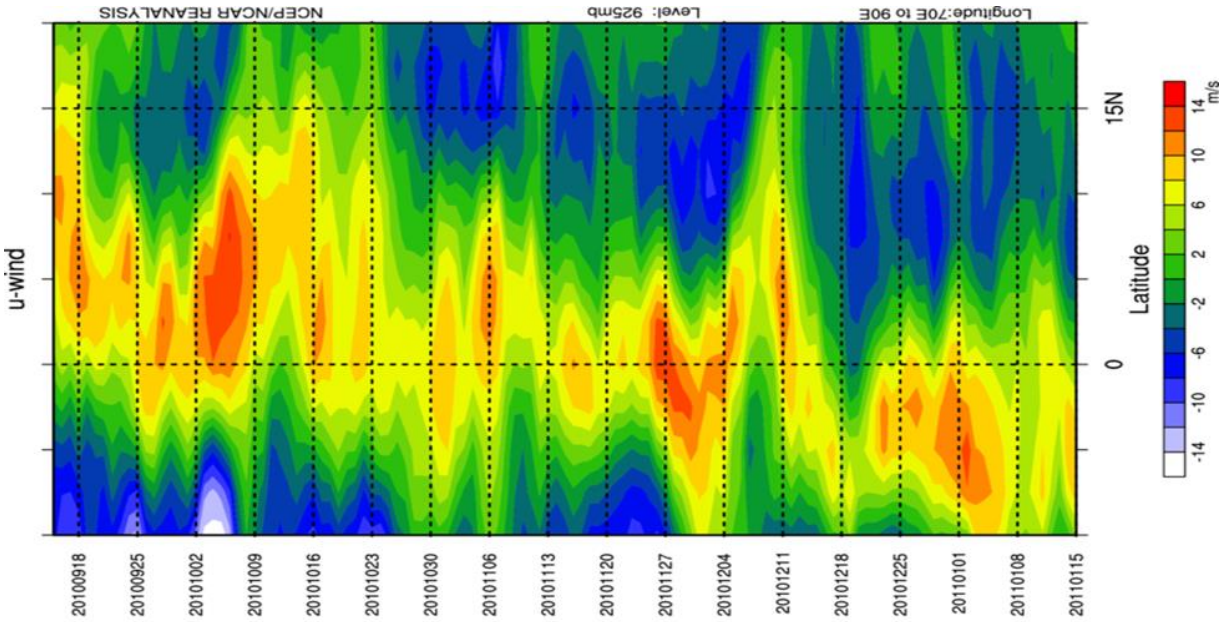


Fig. 6.5 b. Hovmuller diagram (Time vs Latitude) of zonal wind (m/sec) at 925 hPa from 15 September 2010 to 15 January 2011.

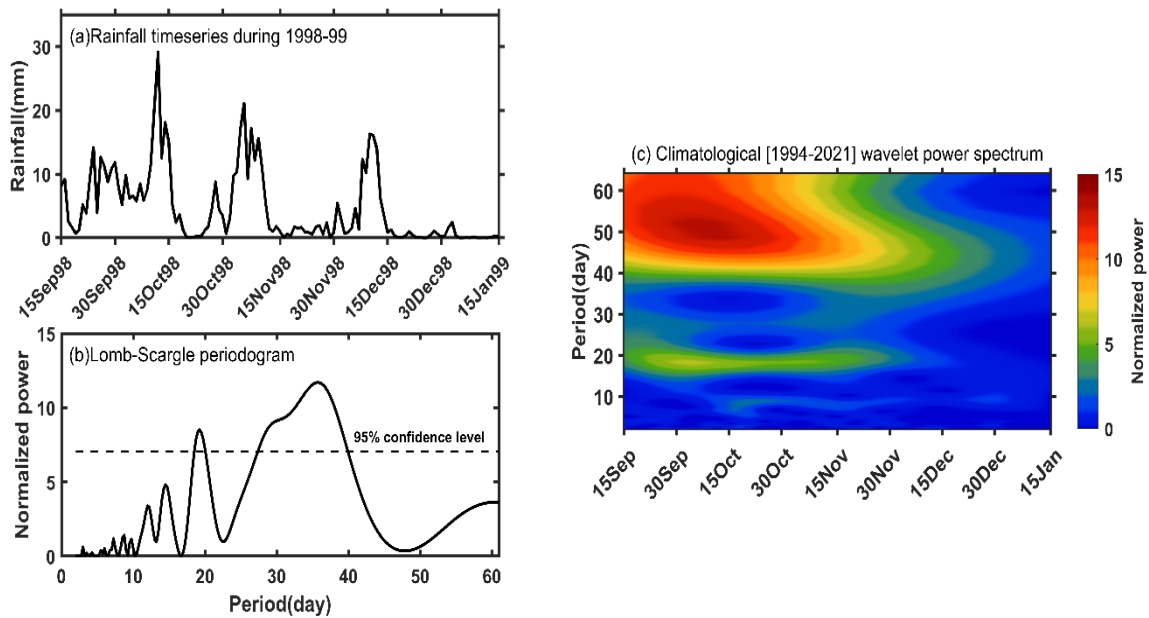


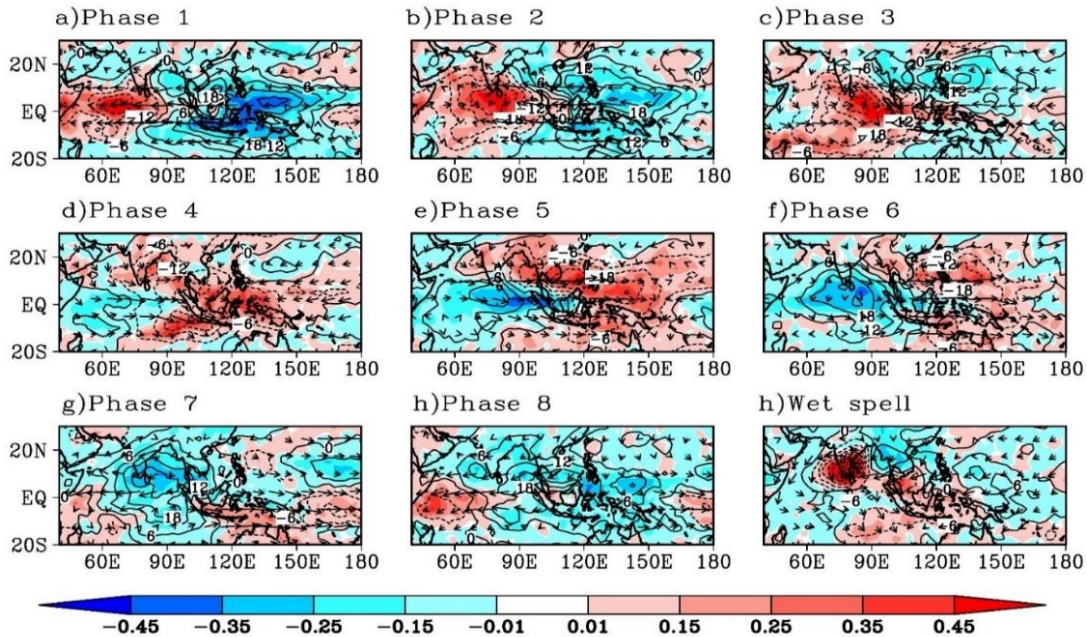
Fig. 6.6. Daily rainfall (in mm) averaged over south Peninsular India from 15 September 1998 to 15 January 1999, b) Lomb-Scargle periodogram of daily rainfall over south Peninsular India from 15 September 1998 to 15 January 1999 and c) wavelet power spectrum of climatological daily rainfall averaged over south peninsular India (1994-2004).

Maps of composite rainfall anomaly (mm) in respect of eight strong phases of MJO superimposed with composite daily OLR anomalies ( $W/m^{-2}$ ) and composite surface wind vector in the eight strong MJO phases were prepared using the data for the period 1979–2021. The results are shown in Fig. 6.7. Positive rainfall anomaly over south peninsular India and the surrounding Indian Ocean (IO) is observed during the strong MJO phases 2, 3 and 4; and negative rainfall anomaly during the strong MJO phases 6,7 and 8. Therefore, an understanding of the phase of MJO (which is available on real time at <http://www.bom.gov.au/>) is useful for assessing the prospects of NE monsoon rainfall over the south Peninsula. From Fig. 6.7, it is very clearly seen the northeastward movement of positive rainfall anomalies from the equatorial Indian Ocean to the west Pacific and neighborhood.

Shanmugasundaram et al. (2017) employed hidden Markov model to characterize the spatio-temporal variations of NE monsoon rainfall at pentad time step and its probability of occurrence during 1982–2014. The results indicated the dominant presence of three rainfall states during the season, which were the wet (State-1), coastal wet (State-2), and dry (State-3) states. Seasonal total NEIMR was significantly and positively correlated with the frequency of State-1, whereas it was negatively correlated with that of State-3, indicating a crucial role of the rainfall states in determining water requirements in the southeastern peninsular India. Wet conditions were characterized by enhanced cyclonic activities and increased moisture convergence at 850 hPa over the southeastern peninsular India and its neighbouring oceanic regions (Bay of Bengal and Indian Ocean).

In contrast, dry conditions were associated with anticyclonic circulation and reduced moisture convergence at 850 hPa. The study by Somenath Dutta et al. (2016) revealed that the transition from weak phase to strong phase of north-east monsoon is associated with an enhancement in conversion of zonal potential energy to zonal kinetic

energy, implying a strengthening of Hadley circulation, favouring the above transition. It is also observed that the transition from weak phase to strong phase is associated with enhanced baroclinic energy conversion.



GrADS/COLA

Fig. 6.7. Maps of composite rainfall anomaly (mm) (shaded) in respect of eight strong phases of MJO superimposed with composite daily OLR anomalies ( $W/m^2$ ) (lines) and composite surface wind vectors in the eight strong MJO phases and during wet spell using the data for the period 1979–2021.

### 6.2.1. Active and Weak Spells of NE Monsoon

Understanding of the intra-seasonal aspects of the NE monsoon is very important for prediction of rainfall. It is well known that the southwest monsoon season exhibits strong active and break spells during the season, and extensive analyses of monsoon active and break spells have been made. During southwest monsoon season, there are active and break spells, with specific characteristics (Ramaswamy 1969, Gadgil and Joseph, 2003 and Rajeevan et al. 2010). It was shown that the total number of active

and break spells during the season is statistically well correlated with the monsoon seasonal rainfall (Rajeevan et al. 2010). Larger number of break spells during the season could lead to a deficient monsoon. However, similar studies of active and break spells during the NE monsoon are unavailable. Since the earlier discussions suggest that there is strong intra-seasonal activity during the NE monsoon season, it is important to understand the active and break spells during the NE monsoon season. A similar analysis of active and weak spells during the NE monsoon season was carried out and the results are discussed below.

Using the IMD gridded daily rainfall data, an area averaged ( $8-14^{\circ}$  N,  $80-85^{\circ}$  E) daily rainfall time series is prepared from 01 Oct to 31 Dec. Using the daily rainfall data, standardized rainfall is calculated for all these days from 1981-2021. An Active (wet) Spell is considered when the area averaged standardized rainfall is more than 1.0 for consecutively three days. Similarly, the weak (dry) spell is considered when the area averaged standardized rainfall is less than -0.8. The asymmetry in the threshold of standardized rainfall anomaly was made to ensure active and weak spell days are similar on a long-term climatological data. Using these criteria, active and weak spells during Oct-Dec are identified for the period 1981-2021. These criteria are similar to the criteria for the active and break events adopted for the southwest monsoon season (Rajeevan et al. 2010).

Table 6.1 shows the active and weak spell days during the period 1981-2021, identified using the above criteria.

The time series of total number of active and weak days during the season, year-wise is given in Fig. 6.8. The mean number of active (weak) days during the season is 7.07 (6.56) with a standard deviation of 5.89 and 6.08 respectively. The standard deviation of active and weak spells is very large. There are few years in which there is neither active nor weak spells. In 2003, maximum number of active days (24) was observed. In 1988 and 2016, maximum number of weak days (20) was observed. As

observed during the southwest monsoon season, total number of active and weak spells during the season influence the NE Monsoon seasonal rainfall. The correlation coefficient between the active and weak days during the season with the seasonal rainfall is 0.447 and -0.603 respectively, which are statistically significant at 95% significance level. Total number of weak days is more correlated with the seasonal rainfall, compared to the total number of active days.

**Table 6.1**  
**Active and Weak Spells during the NE Monsoon Season (Oct-Dec).**  
**Period 1981-2021**

Year	Active Days	Weak Days
1981	25-28 Oct, 02-04 Nov	11-17 Oct, 21-23 Nov
1982	26-28 Oct, 03-05 Nov	01-13Oct
1983	21-27 Dec	11-13Nov
1984	NIL	16-20 Oct, 31 Oct-4Nov
1985	01-03 Oct, 05-11 Oct	19-23 Oct
1986	05-07Nov,12-14Dec	20-25 Oct
1987	16-20 Oct	
1988	22-25Dec	11-18 Oct, 20-23 Oct, 27-31 Oct, 21-23Nov
1989	NIL	03-05 Oct, 14-16 Oct
1990	25-28Oct, 31Oct-2Nov,15-17Dec, 28-31Dec	7-9 Nov
1991	29-31Oct,15-18Nov,24-26Dec	NIL
1992	13-18 Nov,	20-31 Oct
1993	8-12Nov, 4-7 Dec	NIL
1994	04-06 Oct,7-9 Dec ,27-29 Nov	NIL
1995	NIL	NIL
1996	02-05 Oct,18-20 Oct,9-11 Dec, 13-17Dec	2-6 Nov
1997	8-10Nov, 24-30 Nov, 4-10 Dec	07-9 Oct
1998	11-18Oct, 7-10 Nov,8-12 Dec	NIL
1999	5-8Oct, 21-23 Nov	1-3Nov
2000	NIL	25-27 Oct,30Oct-9Nov
2001	NIL	NIL

2002	13-16 Oct	1-8 Oct,21-25 Oct
2003	6-8 Oct,21-24 Oct,1-17 Dec	11-13 Oct,15-17oct,2-6Nov
2004	3-5 Oct	3-5 Nov
2005	12-15 Oct,22-25 Nov	6-8 Oct
2006	26-30oct,4-6dec	12-14 Oct
2007	19-21 Dec	9-13 Oct
2008	24-30 Nov,19-21 Dec	1-3 Oct, 29 Oct-7 Nov
2009	1-5 Oct, 5-12 Nov, 14-16 Nov	10-12 Oct ,14-28 Oct
2010	31Oct-2 Nov ,17-19 Nov,21-23 Nov, 7-9 Dec	11-14 Oct
2011	NIL	1-3 Oct, 5-9 Oct,18-21 Oct, 21-23 Nov
2012	1-3 Nov	8-10 Oct,26-28 Oct
2013	22-26 Oct	9-11 Nov
2014	26-28 Oct	2-5 Oct
2015	30 Nov-3 Dec	16-18 Oct,21-24 Oct
2016	NIL	15-20 Oct,22-29 Oct, 6-8 Nov,11-13Nov
2017	NIL	17-19 Oct,23-26 Oct
2018	NIL	26-31 Oct,6-8Nov
2019	19-22 Oct, 24-26 Oct, 30Nov-3Dec, 13-15 Dec	NIL
2020	11-15 Oct,16-18 Nov, 3-5 Dec,7-9 Dec,	30 Oct-2 Nov
2021	17-19 Oct,12-15 Nov,18-21 Nov	NIL

To understand better the active and weak spells during the NE monsoon season, an analysis is made to make the composites of circulation and SST anomalies for the active and weak spells using the days of active and weak spells mentioned in Table 6.1. The results are discussed below.

Fig. 6.9 shows the composite rainfall anomalies during the active and weak spell days, calculated using the rainfall data of ERA5. Fig. 6.9 shows large positive (negative) anomalies over the south peninsula during the active (weak) spell days. Over the equatorial south Indian Ocean and the west Pacific, there are sharp differences between the active and weak spell days. An active (weak) spell is also associated with suppressed (enhanced) rainfall activity over the west Pacific and the equatorial Indian Ocean.

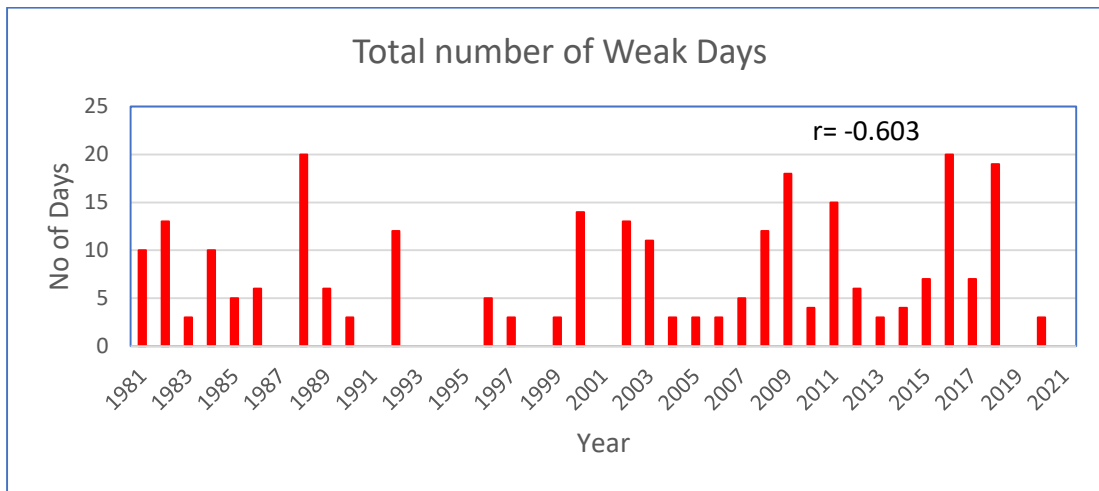
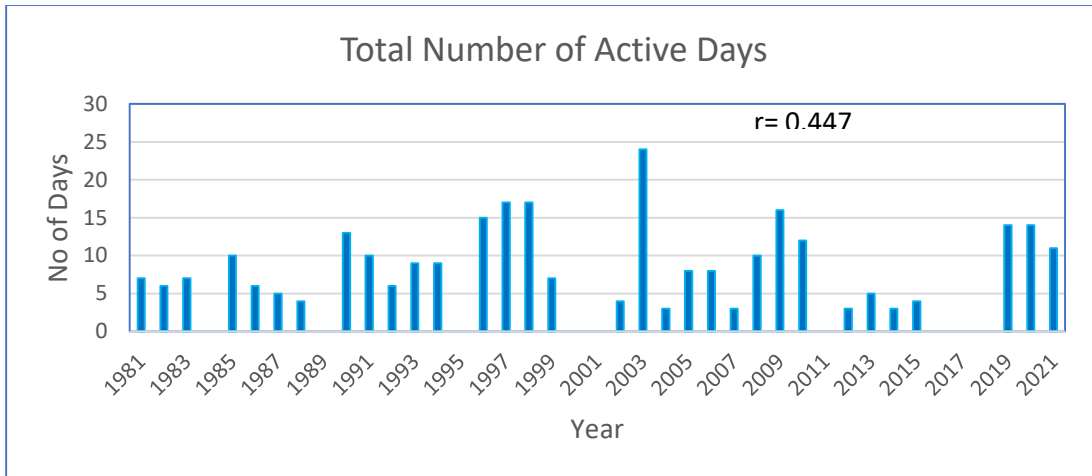


Fig. 6.8. Total number of active (above) and weak (below) days during the OND season for different years, 1981-2021. The correlation coefficient between the total number of active and weak days with the seasonal rainfall is shown in the plots.

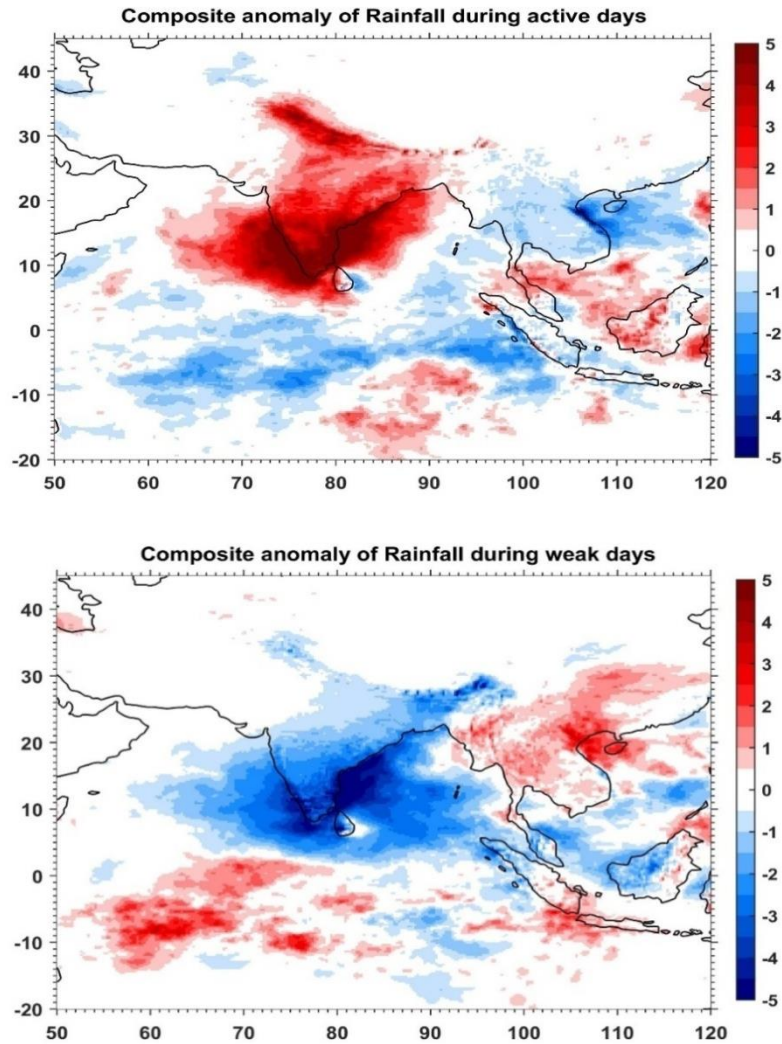


Fig. 6.9. Composite rainfall anomalies (mm) during the active spell days (above) and weak spell days (below) for the period 1981-2021.

Fig. 6.10 shows the composite SST anomalies during the active and weak spell days. The largest differences between the active and weak spells are observed over the equatorial Pacific and the north Indian Ocean. Over the equatorial Pacific Ocean, the SST anomalies are positive (negative) during the active (weak) spells. This indicates that enhanced rainfall activity (more active days) is observed during the El Nino years. Similarly, during the La Nina years, the weak spell days are more. During the active (weak) spell days, SST anomalies over the equatorial Bay of Bengal and Arabian Sea are

large negative (positive). However, over the north Bay of Bengal, positive (negative) anomalies are observed during the active (weak) spell days.

Fig. 6.11 shows the similar composite plots, but for the OLR anomalies. The results are consistent with the rainfall anomaly plots. During the active (weak) spell days, OLR anomalies are large negative (positive) over the Indian sub-continent suggesting enhanced (suppressed) rainfall activity. The drastic difference between these two cases is observed over the west Pacific Ocean and China and adjoining area. During the active (weak) phase of the monsoon, convection over the west Pacific is suppressed (enhanced). The enhanced convection over the west Pacific could cause anomalous descending motion over the Indian region and thus reduce the NE monsoon activity.

Fig. 6.12 shows the 850 hPa wind anomalies during the active and weak spells of NE monsoon. The most striking feature of the wind anomalies is observed over the Indian region. The active (weak) phase of the NE monsoon is associated with cyclonic (anti-cyclonic) circulation anomalies over the Indian region, which is consistent with the observed rainfall anomalies. The other significant anomalies are observed over the west Pacific and adjoining eastern parts of China. During the active (weak) phase, an anomalous anticyclonic (cyclonic) circulation is observed over the region, suggesting below (above) normal convection over the region. This is consistent with the OLR anomalies discussed above.

### **6.3. Interannual variation of NE monsoon rainfall (NEMR)**

In this section, the inter-annual variability of NE monsoon rainfall is discussed. There are not adequate studies examining the inter-annual variability of NE monsoon rainfall except the studies by De and Mukhopadhyay, 1999; Kripalani and Kumar, 2004; Raj and Geetha, 2008; Zubair and Ropelewski, 2006; Kumar et al., 2007; Sreekala et al., 2012, Rajeevan et al., 2012.

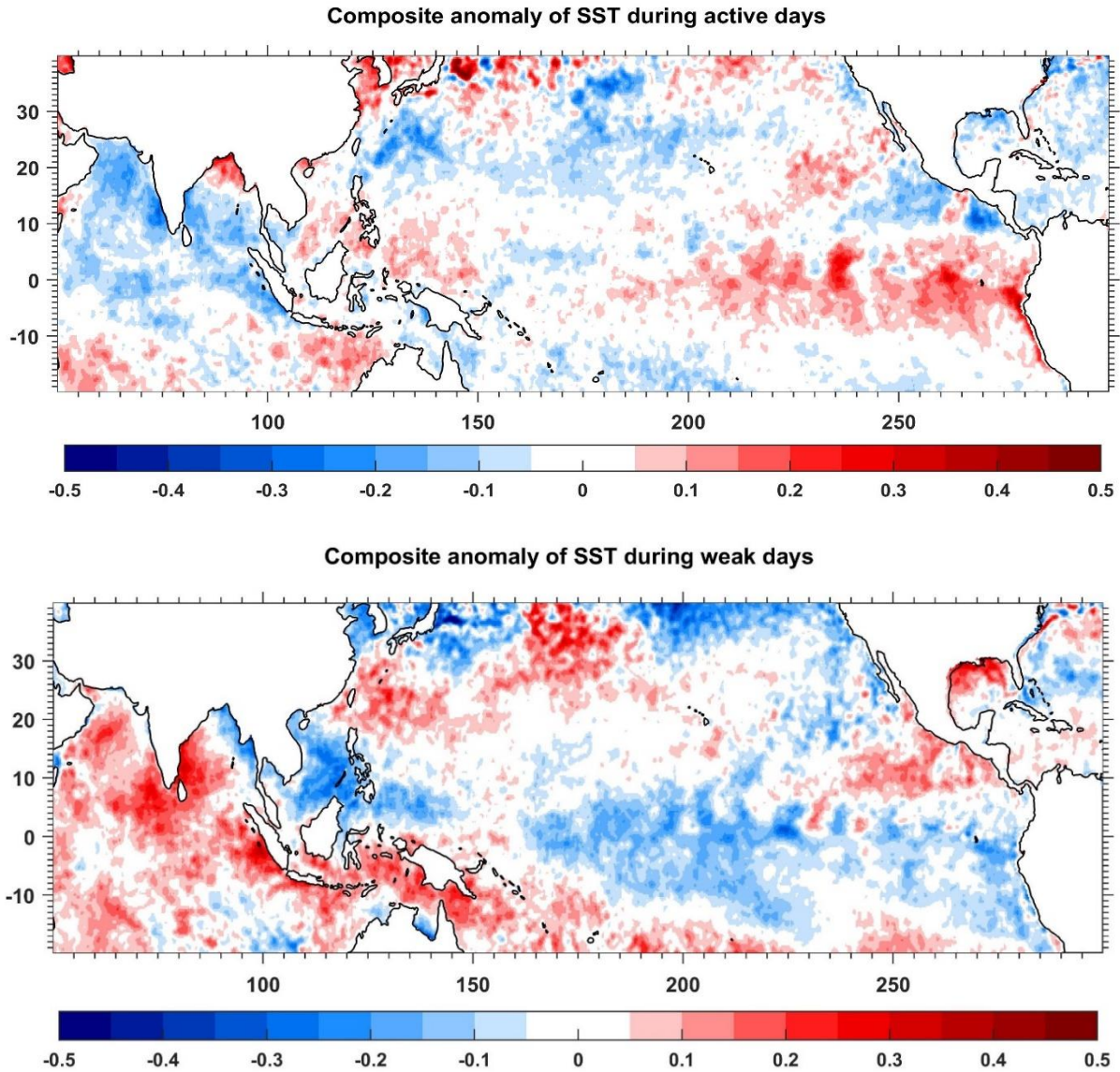


Fig. 6.10. Composite Sea Surface Temperature (SST) ( $^{\circ}\text{C}$ ) anomalies during the active spell days (above) and weak spell days (below) for the period 1981-2021.

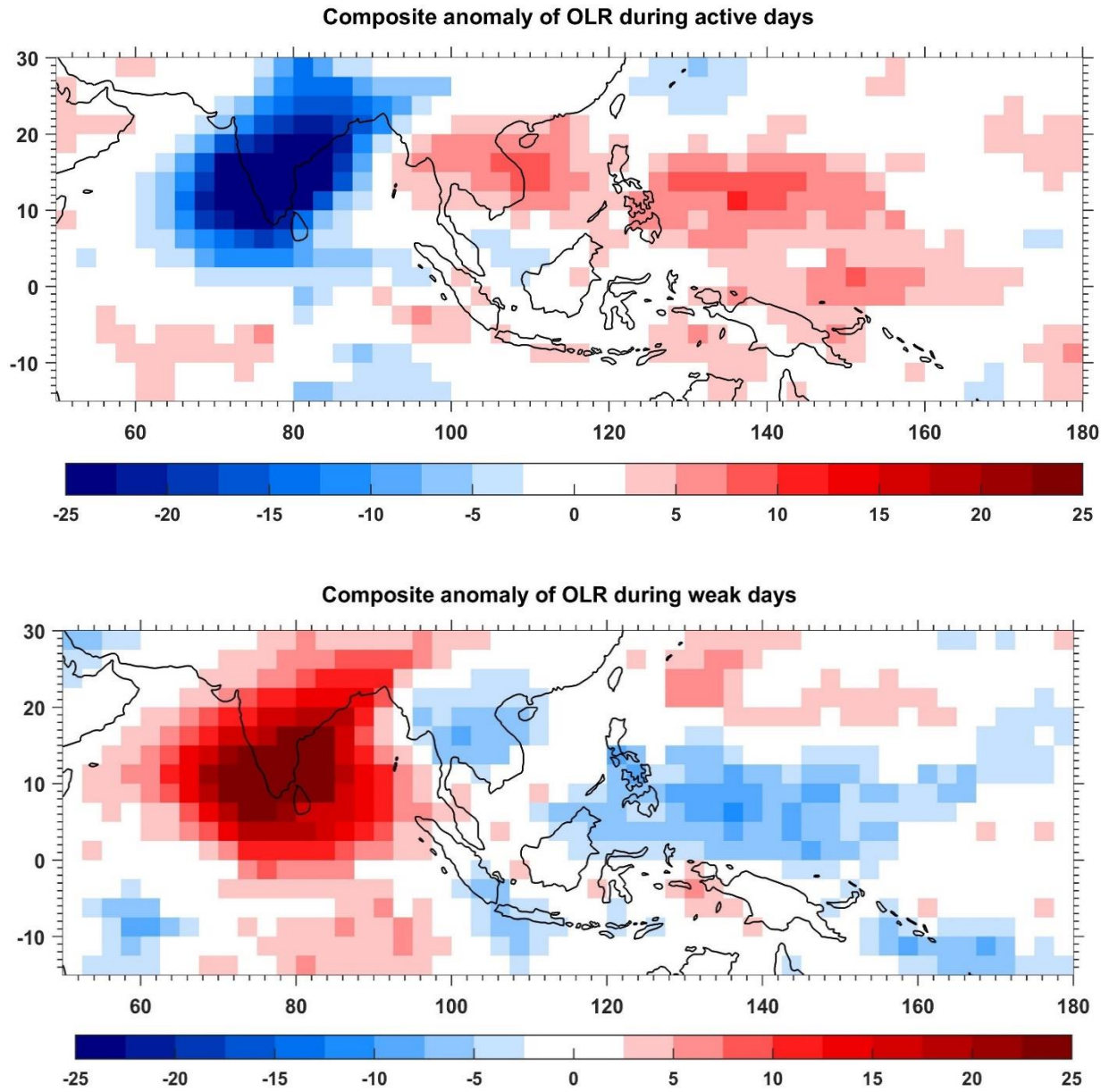


Fig. 6.11. Composite OLR anomalies ( $\text{Wm}^{-2}$ ) during the active spell days (above) and weak spell days (below) during the period 1981-2021.

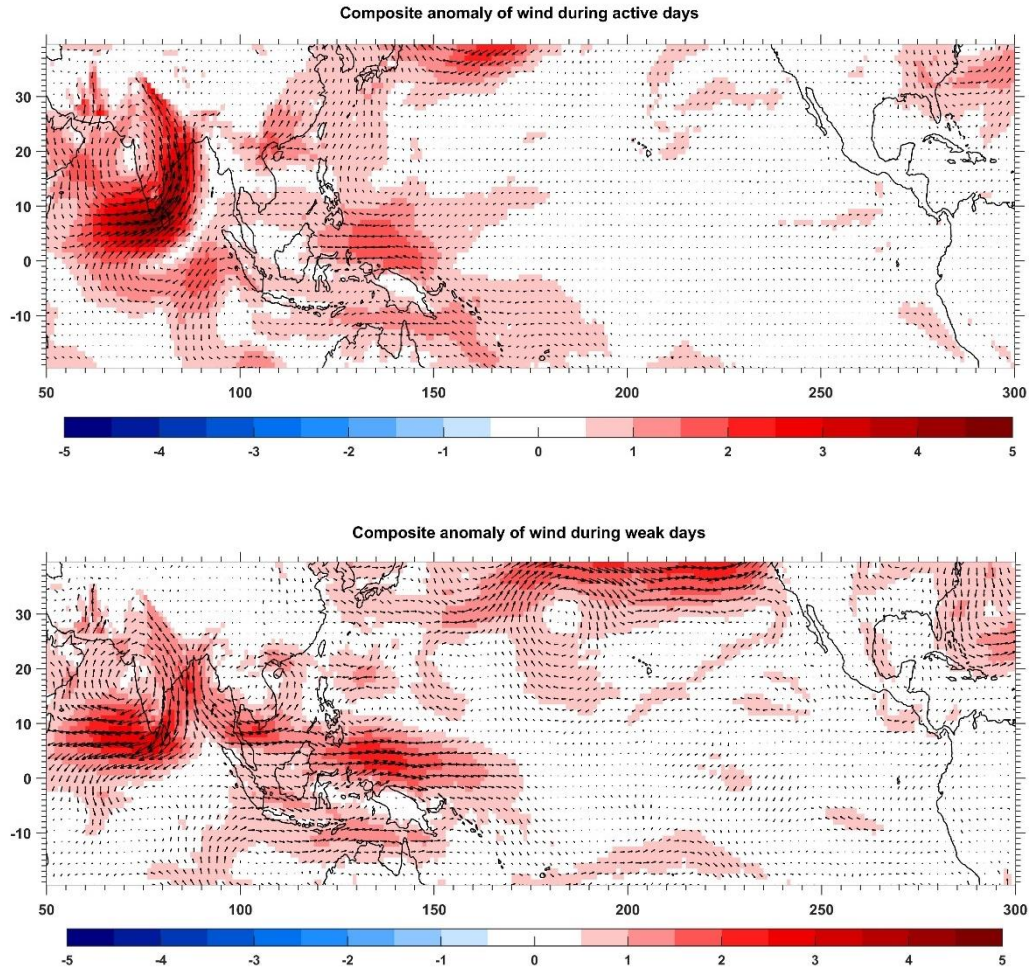


Fig. 6.12. Composite OLR anomalies ( $\text{Wm}^{-2}$ ) during the active spell days (above) and weak spell days (below) during the period 1981-2021.

The inter-annual variability of the NEMR is calculated using the sub-divisional rainfall data for the period 1901–2021. During the northeast monsoon season, south peninsular India receives a mean rainfall of 338.4 mm with a coefficient of variation of about 25%. It may be noted that the coefficient of variation during the NE monsoon season is much more than that of SW monsoon rainfall (June to September) for the whole country which is around 10%.

Fig. 6.13 a shows the interannual variation of the NEMR as expressed as percent departure of the seasonal rainfall. No long-term trend in the NEMR is noticed, but there

are years with large rainfall departures, even exceeding 40%. The years with more (less) than 1 Standard Deviation (25%) are termed as excess (deficient) years. If the departure is more than -25% but less than 25%, then those years are termed as normal years. Out of 121 years (1901-2021), there were 78 normal years, 23 excess years and 20 deficient years. Among these years, the 2021 monsoon season has the highest positive departure (73%). The year 2016 was the worst deficient year with a deficiency of 65%. The other two notable excess years are 2010 and 2015. The other two notable deficient years are 1938 and 1988. Recently, three consecutive years 2016-2018 experienced below normal rainfall with large negative rainfall departures. However, the subsequent three years witnessed above normal monsoon rainfall with positive departures. Fig. 6.13 b shows the 21-year moving average of the NEMR during the period 1901–2021. It clearly shows the multi-decadal variations of the NEMR with epochs of above normal and below normal rainfall. An increasing trend in the NEMR during the recent years is observed.

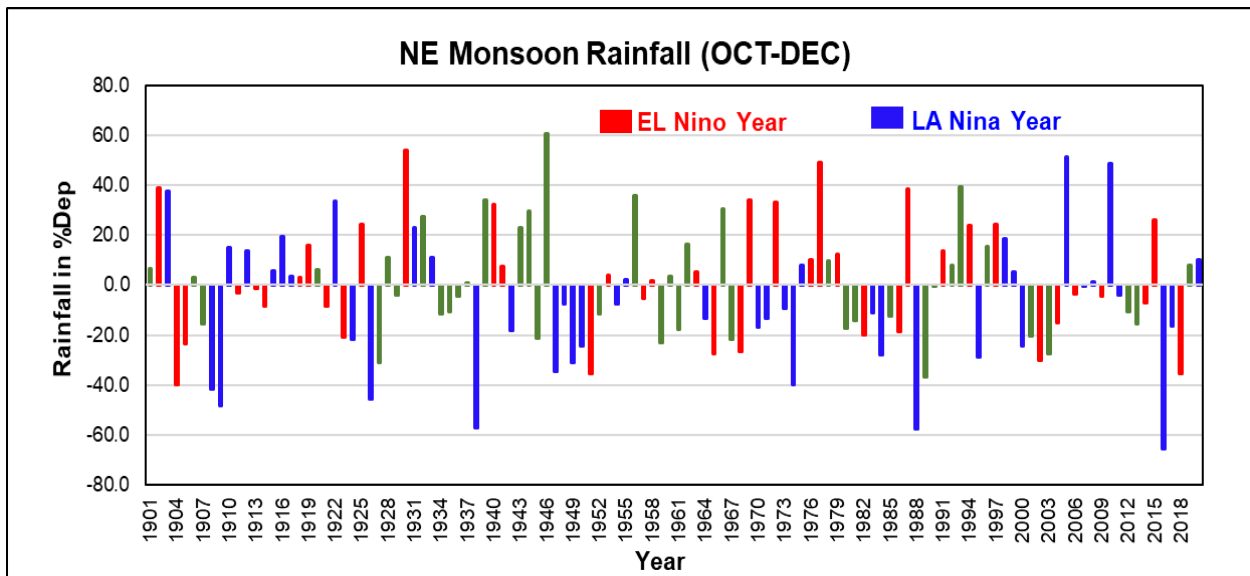


Fig. 6.13 a. Time series of NE monsoon seasonal rainfall as % Departure from 1901-2020. El Nino year is shown as red and La Nina year is shown as blue lines.

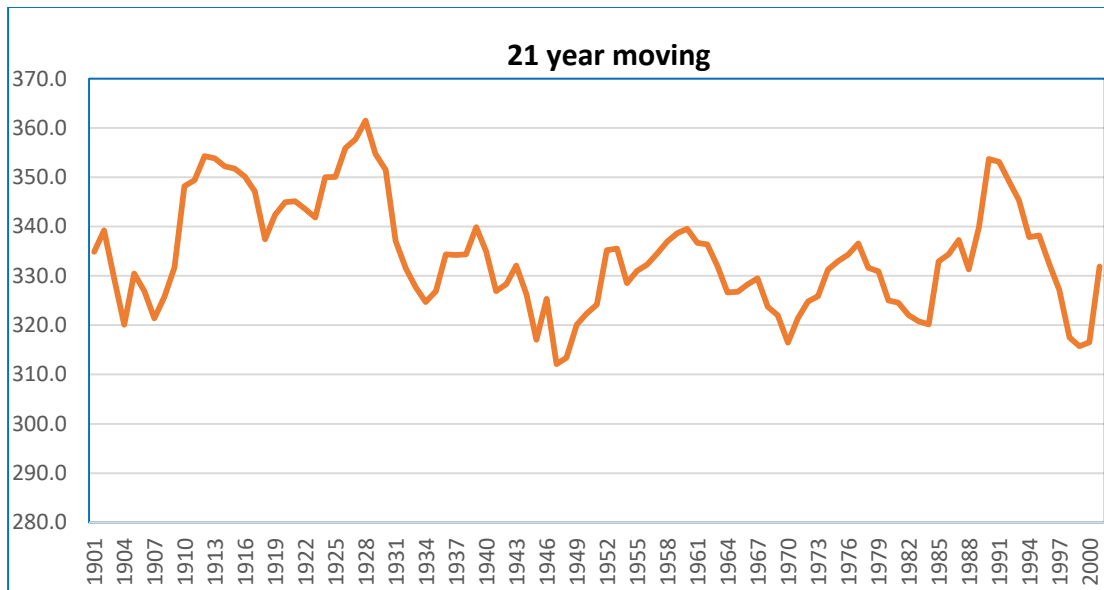


Fig. 6.13 b. The 21 year moving mean of NE monsoon seasonal rainfall (Oct-Dec) in mm, showing multi-decadal variations of NE monsoon rainfall.

Fig. 6.14 a shows the periodogram of NE Monsoon seasonal rainfall for the period 1901-2021. Even though many periodicities of shorter duration are seen, the periodicity of about 16 years is close to the significant (90% significance) level. Fig. 6.14 b shows the wavelet spectrum of NE monsoon seasonal rainfall for the same period 1901-2021. It clearly shows the periodicity of about 16 years, which is statistically significant. This periodicity, however, was not uniformly active during the whole period. It was active till about 1950. Then, it became active from 1980s till date. Raj (2012) also suggested the periodicity of similar periods for NE monsoon rainfall. This periodicity is also apparent in the 21-year running mean shown in Fig. 6.13 b. The periodicity of 2-3 years (quasi biennial) is observed during 1920s to 1970s. Kripalani and Kumar (2004) also suggested the NE monsoon rainfall undergoes different epochs of above and below normal rainfall. These epochs last about a decade or two. More studies are required to understand the decadal variations of NE monsoon rainfall using long term data.

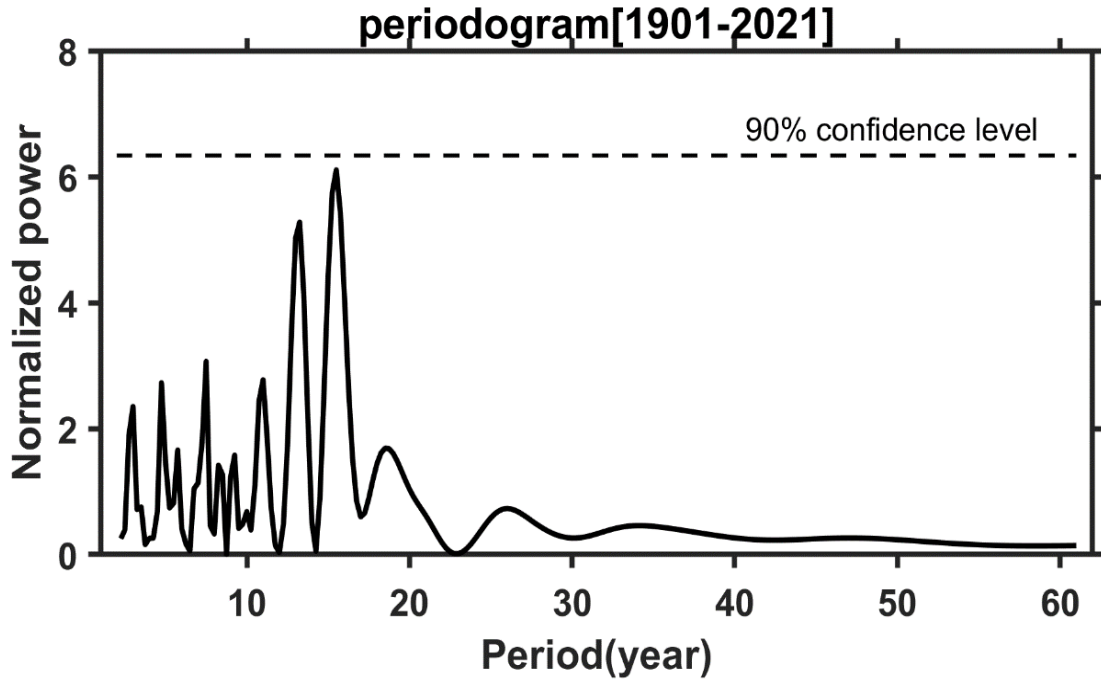


Fig. 6.14 a. Periodogram of NE Monsoon seasonal rainfall (1901-2021). The peak around 16 years is close to significance level at 90%.

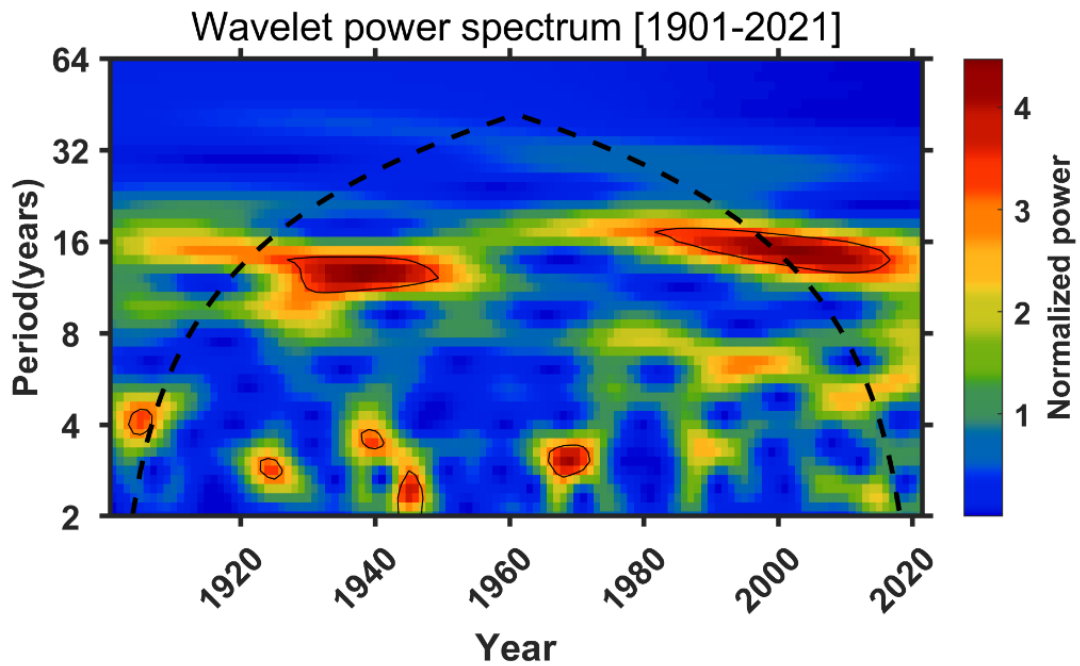


Fig. 6.14 b. Wavelet power spectrum (1901-2021) of NE monsoon seasonal rainfall. The periodicity close to 16 years is statistically significant.

The inter-annual variability of the NEMR is linked to the El Nino/Southern Oscillation (ENSO), the Indian Ocean Dipole and the EQUINOO (De and Mukhopadhyay, 1999; Kripalani and Kumar, 2004; Raj and Geetha, 2008; Jayanthi and Govindachari 1999; Zubair and Ropelewski, 2006; Kumar et al. 2007; Sreekala et al. 2012, Rajeevan et al. 2012). ENSO is an irregular periodic variation in Sea surface temperatures and winds over the equatorial Pacific Ocean. ENSO influences the climate of much of the tropics and subtropics. ENSO is a coupled process in which the equatorial Pacific and atmosphere interact. The warming phase of the sea surface temperature is known as El Nino and the cooling phase as La Nina. The Southern Oscillation is the accompanying atmospheric component, coupled with the changes in SST.

The Indian Ocean Dipole (IOD) is defined by the difference in sea surface temperature between two areas – a western pole in the Arabian Sea (western Indian Ocean) and an eastern pole in the eastern Indian Ocean south of Indonesia. The IOD affects the climate of Australia and other countries surrounding the Indian Ocean Basin, and is a significant contributor to rainfall variability in this region. Positive Dipole events are characterized by positive (negative) SST anomalies over the west (east) equatorial Indian Ocean. Conversely, the negative phase is characterized by negative (positive) SST anomalies over the west (east) equatorial Indian Ocean.

Fig. 6.15 a shows the spatial pattern of correlations between Oct-Dec SST and NE monsoon rainfall during two 30-year periods, 1961-1990 and 1991-2020. The plot for the period 1961-1990 clearly shows that positive SST anomalies over the equatorial Pacific Ocean (El Nino) are associated with normal or above normal rainfall. However, during the recent 30-year period, the positive correlations over the equatorial Pacific have weakened. Another interesting area of strong correlation is over the North Atlantic. During the period 1961-1990, strong positive correlations are observed, which are replaced by weak negative correlations during the period 1991-2020.

Raj and Geetha (2008) analyzed the relationship between Southern Oscillation Index (SOI) and NE monsoon rainfall in antecedent and concurrent mode and found there is a negative relationship. The relationship in antecedent mode is stronger. Sengupta and Nigam (2019) studied the aspects of ENSO impact on NE monsoon rainfall. Their study suggested stronger NE monsoon rainfall over south peninsula and Sri Lanka during El Nino events. The impact varies sub-seasonally, being weak in October and strong in November. The positive anomalies over the south peninsula are generated by anomalous anticyclonic flow centered over the Bay of Bengal, which is forced by an El Nino-related reduction in deep convection over the Maritime continent.

In fact, the correlation between NE monsoon rainfall and Nino 3.4 changes its sign by middle of October. Till middle of October, the correlation is negative and it changes to positive correlation by November. Fig. 6.15 b clearly suggests this shift in the sign of correlation between Nino 3.4 and NE monsoon rainfall by October end.

However, the relationship between NE monsoon and ENSO is not very stable. It was weakened during the recent epoch (1991-2020) (Fig. 6.15 c). Another interesting aspect to be noticed is the positive correlation of SSTs over the north Bay of Bengal with the NE monsoon rainfall, suggesting a warmer Bay of Bengal could be related to better performance of NE monsoon rainfall. It may be interesting to examine long term data to understand why the relationship between ENSO and NE Monsoon rainfall undergoes secular variations.

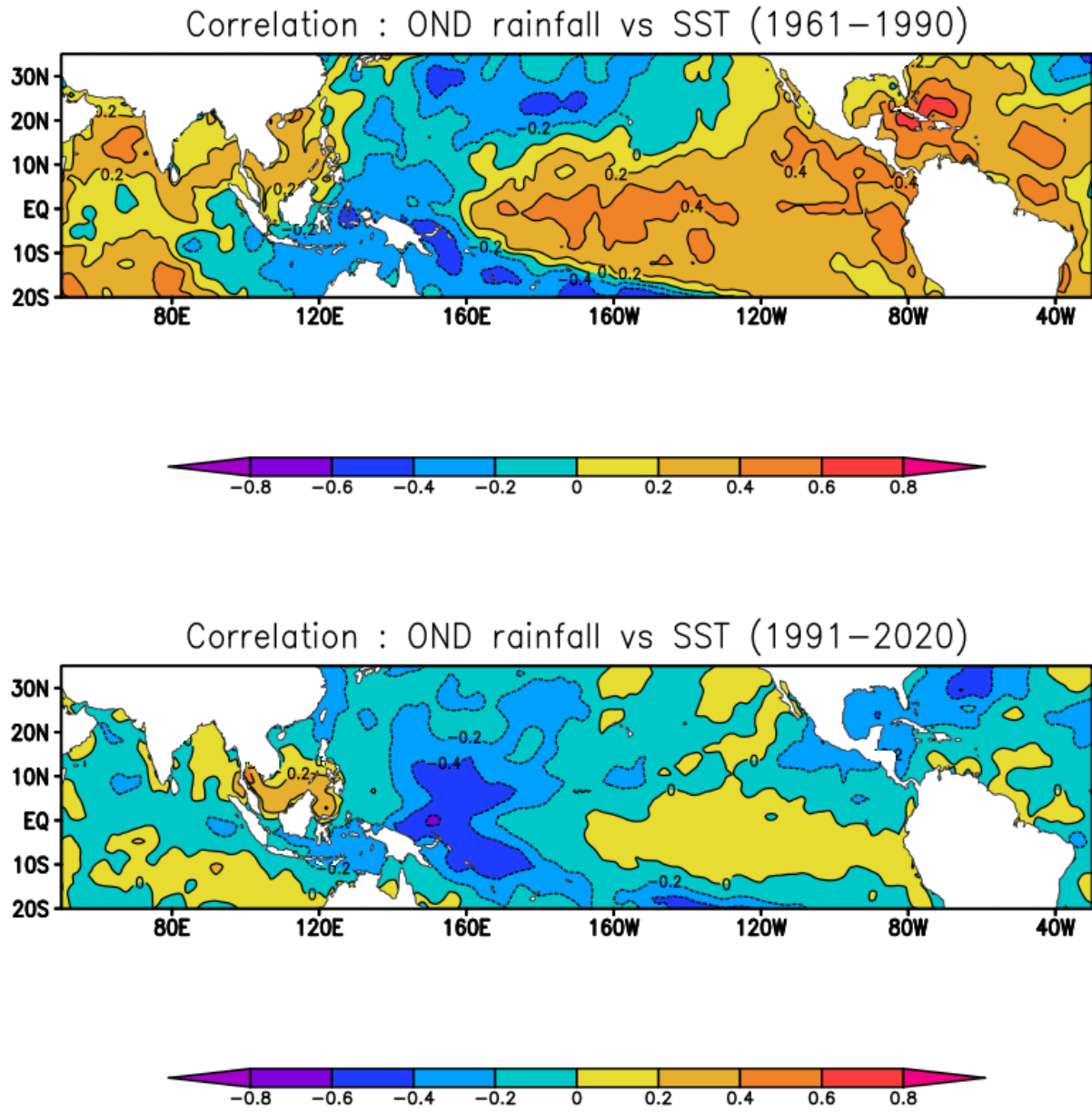


Fig. 6.15 a. Spatial Pattern of correlation between Sea Surface Temperature (SST) and NE Monsoon seasonal rainfall during the period 1961-1990 (above) and 1991-2020 (below).

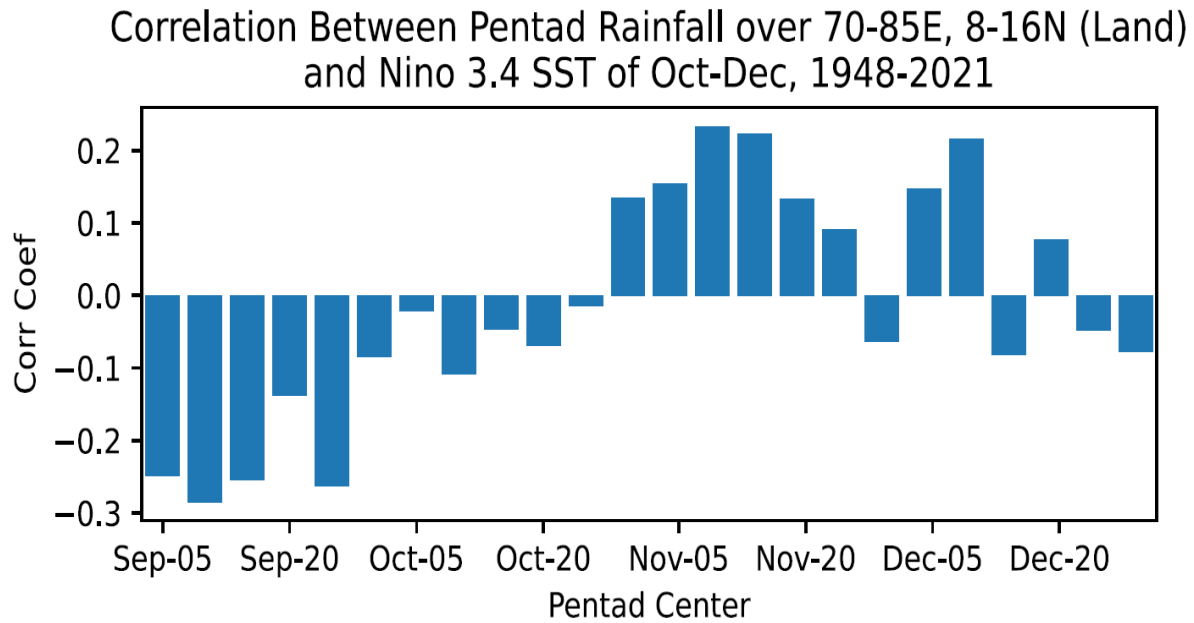


Fig. 6.15 b. Correlation between pentad rainfall averaged over south peninsula and Nino 3.4 SST index. The period 1948-2021 is considered for the analysis.

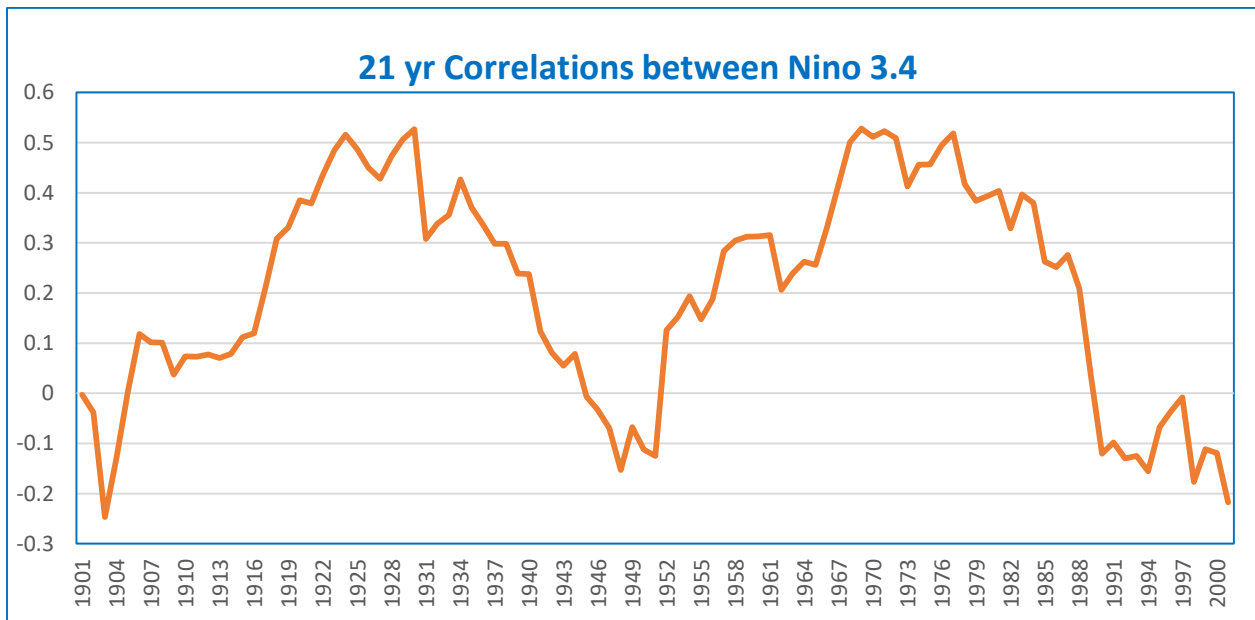


Fig. 6.15 c. The 21 year moving correlations between Nino 3.4 index during OND and NE Monsoon seasonal rainfall (OND) suggesting multi-decadal variation of relationship between NE monsoon rainfall and El Nino.

Table 6.2 below shows El Nino/La Nina's relationship with NE monsoon rainfall.

**Table 6.2**  
 Relationship between ENSO and NE Monsoon Rainfall  
 Period: 1940-2021

El Nino Years (39)			La Nina Year (42)		
Excess >25%	Normal -25% to 25%	Deficient < -25%	Excess >25%	Normal -25% to 25%	Deficient < -25%
11	22	6	6	23	13
28%	57%	15%	14%	55%	31%

The analysis shows that the probability of an El Nino year being an excess NEMR year is higher (28%) compared to the year being a deficient (15%) monsoon year. However, the probability of a La Nina year being an excess monsoon year (14%) is smaller compared to an excess (31%) monsoon year. Therefore, more confidence in excess or deficient monsoons may be obtained with the additional information on IOD. However, compared to the Southwest monsoon, the NE monsoon is not very strongly related to ENSO or IOD.

An analysis was carried out by Prasanna et al. (2019) of two successive La Niña years, referred to as the first and second year during the period 1900–2010 to see the impact on NE monsoon rainfall. Observations show that despite noticeable weakening in the equatorial Pacific cooling from the first year to the second year, strong La Niña teleconnections and the rainfall deficiency over the region remains the same in most of the multiyear-La Niña events (70%).

Even though, there is a high probability for NE monsoon to be on lower side of the normal during the La Nina years, there have been three major exceptions to be examined in detail. These years occurred recently, 2010 and 2021, when the ENSO-NE

monsoon rainfall relationship was weaker. The NE monsoon rainfall percent departure during these three seasons was 49% and 73% respectively. The year 2021 was truly an exception.

Kripalani and Kumar (2004) documented the NEMR and IOD relationship. They suggested that the NEMR variability is enhanced during the decades when the IOD exhibits its active phase, and is suppressed during the decades when the IOD is inactive. This relationship suggests that the positive (negative) phase enhances (suppresses) the northeast monsoon activity. During the positive phase, the anomalous flow pattern shows winds converging and suggesting moisture transport from the southeast Indian Ocean and the Bay of Bengal towards south peninsular India. In contrast, the negative phase reveals winds diverging and transporting moisture away from the south Indian region. These results show the direct influence of the IOD phenomenon on the interannual NE monsoon rainfall variability over south India.

Balachandran et al. (2006) examined the local and teleconnective association between Northeast Monsoon Rainfall over Tamil Nadu and global surface temperature anomalies (STA) using the monthly gridded STA data for the period 1901–2004. It is observed that the meridional gradient in surface air temperature anomalies between Europe and north Africa, in the month of September is directed from the subtropics (higher latitudes) to higher latitudes (subtropics). It is also observed that North Atlantic Oscillation (NAO) during September influences the surface air temperature distribution over north Africa and Europe. Also, the NAO index in January shows significant inverse relationship with the NE monsoon rainfall since recent times. The central and eastern equatorial Pacific oceanic regions have significant and consistent positive correlation with NE monsoon rainfall while the western equatorial region has significant negative correlation with Northeast monsoon rainfall. A zonal temperature anomaly gradient index (ZTAGI) defined between eastern equatorial Pacific and western equatorial Pacific shows stable significant inverse relationship with Northeast monsoon rainfall.

The unusual excess year of the 2021 NE monsoon season is discussed below.

#### **6.4. The unusual NE monsoon during the year 2021**

During the year 2021, the southwest monsoon withdrew from the Indian region on 25<sup>th</sup> October. Simultaneously, the Northeast monsoon (NEM) of 2021 commenced over the southeastern parts of peninsular India on 25<sup>th</sup> October against the normal date of 20<sup>th</sup> October. Excepting Coastal Andhra Pradesh (CAP), which received normal rainfall during the season, the other four sub-divisions [Tamil Nadu (TN (including Puducherry & Karaikal), Kerala (KER), Rayalaseema (RYS) and South Interior Karnataka (SIK)] benefitted from the NE monsoon. These sub-divisions received excess to large excess rainfall during the NEM season (October-December) with KER, SIK, RYS recording more than 100% excess (large excess) rainfall. During the season, there were 30 days of active to vigorous monsoon conditions over Tamil Nadu and Kerala. There were 65 days of isolated heavy rainfall activity with 33 days of isolated very heavy rain, including 09 days of isolated extremely heavy rainfall activity over Tamil Nadu. Two Depressions formed over the North Indian Ocean during November contributed significantly to NEM rainfall over the peninsular India. Cyclonic Storm (CS) Jawad over the Bay of Bengal (BOB) during 02-06 December tracked northwards towards West Bengal- Bangladesh coasts and did not contribute towards NEM seasonal rainfall. However, two days of extremely heavy rainfall occurred over Chennai (i) 06<sup>th</sup> November night & (ii) 30<sup>th</sup> December 2021. Recurrent heavy rainfall over the coastal and adjoining districts from the last week of October to November led to the filling up of water bodies, and inland and riverine flooding occurred over several areas of Tamil Nadu and Rayalaseema. As a result, NE monsoon 2021 was extended into January 2022 and cessation of NEM 2021 rainfall over peninsular India was declared on 22<sup>nd</sup> January 2022 (Geetha et al., 2022). A more detailed report on 2021 NE monsoon is available for reference (Geetha et al., 2022).

The Table 6.3 presents the frequency of active and vigorous monsoon days and heavy rainfall days during the 2021 NE monsoon season (after Geetha et al., 2022).

**Table 6.3**

Subdivision	Number of Days				
	Activity		Heavy Rainfall		
	Vigorous	Active	Extremely Heavy	Very Heavy	Heavy
Tamil Nadu	8	22	9	33	65
Coastal Andhra Pradesh	2	7	0	8	28
Rayalaseema	8	12	1	4	22
Kerala	11	19	2	18	40
South Interior Karnataka	5	10	0	9	28

**Note:** Heavy Rainfall > 6.5 cm/day Very Heavy rainfall> 12 cm/day and Extremely Heavy rainfall >21 cm/day

Active: Fairly widespread to widespread sub-divisional rainfall with rainfall more than 1.5 to 4 times the normal with at least two stations reporting more than or equal 5 cm in coastal Tamil Nadu and south coastal Andhra Pradesh and 3 cm elsewhere in the NEM region.

Vigorous: Fairly widespread to widespread sub-divisional rainfall with rainfall more than 4 times the normal with at least two stations reporting more than or equal to 5 cm in the coastal Tamil Nadu and the south coastal Andhra Pradesh and 3 cm elsewhere in the NEM region.

Fig. 6.16 a shows the seasonal (Oct-Dec) rainfall over the south peninsula and neighborhood (in mm/day) during the 2021 monsoon season. It shows widespread abundant rains over the south Peninsula and the adjoining southwest Bay, suggesting an excess monsoon year (73% above its long period average).

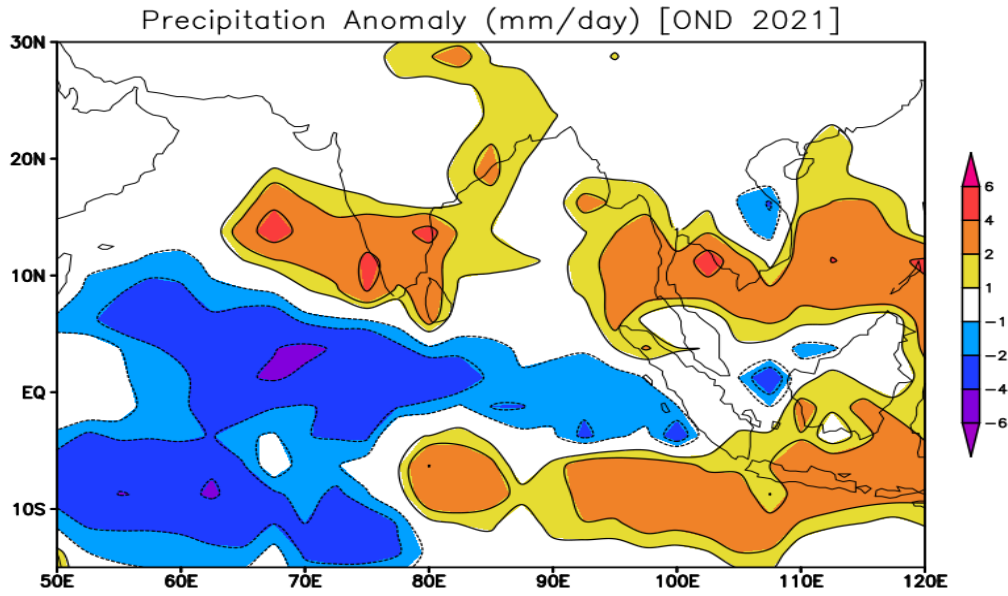


Fig. 6.16 a. Precipitation anomaly (mm/day) during OND 2021. Source: ERA5 reanalysis.

The 850 hPa wind pattern (Fig. 6.16 b) shows an extended east-west trough extending from the east central Arabian sea to the west equatorial Pacific Ocean across the south peninsula and south Bay of Bengal. This suggests the presence of active ITCZ over the region during the NE monsoon season. This convergence zone must be the cause of the genesis of several weather systems over the south Bay of Bengal and their westward movement towards the south Peninsula. The SST anomaly during Oct-Dec 2021 (Fig. 6.16 c) shows the presence of cold SST anomalies over the equatorial Pacific, suggesting La Nina conditions. It may be interesting to note the presence of above normal SSTs over the Bay of Bengal. Some recent studies like Singh et al. (2017) suggested that local air-sea interaction plays a crucial role in modulating or driving extremes over South Peninsula associated with ENSO. More studies are required to understand the physical mechanisms of relationship of Bay of Bengal SSTs and the NE monsoon rainfall.

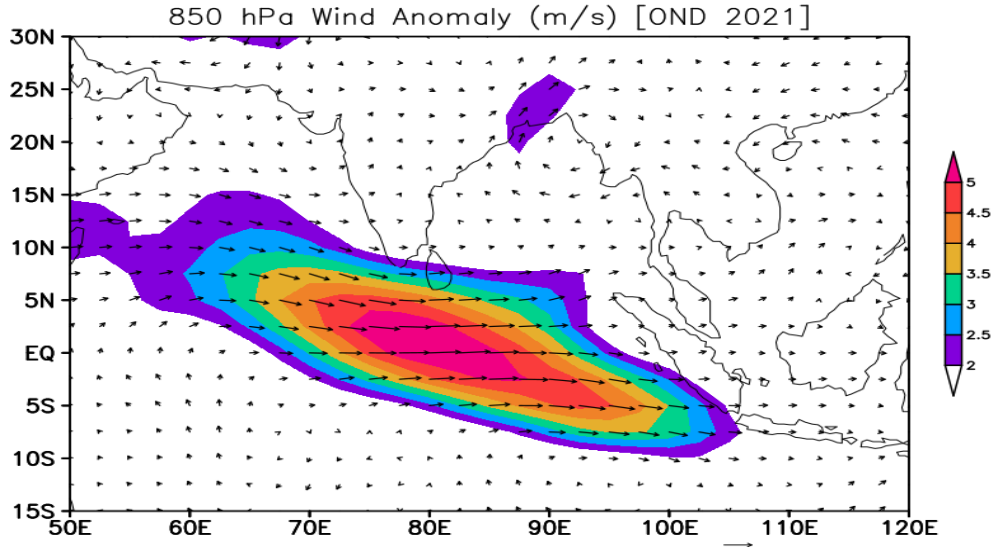


Fig. 6.16 b. 850 hPa wind anomalies during OND 2021. Source: ERA5 reanalysis.

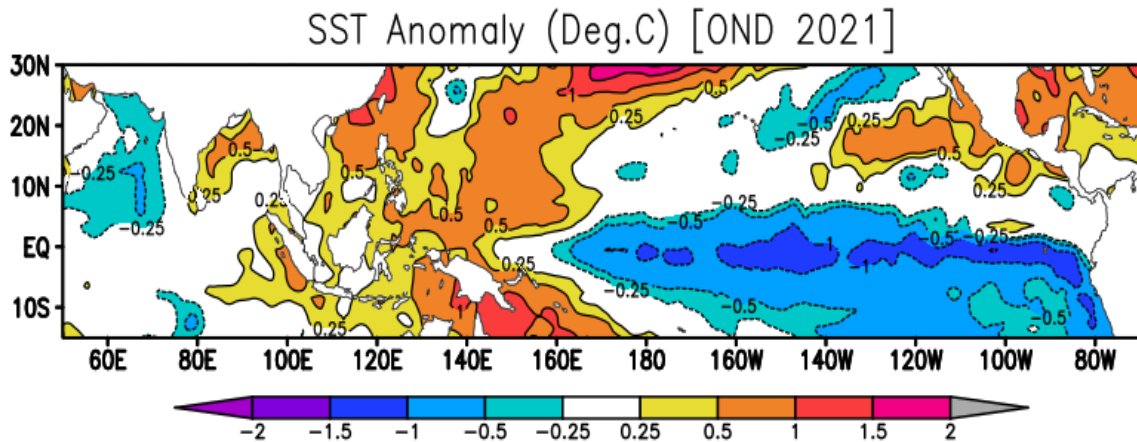


Fig. 6.16 c. SST anomalies during OND 2021. Source: NOAA OI SST data.

### 6.5. Seasonal Forecasting of NE Monsoon

India Meteorological Department (IMD) has been attempting to prepare long-range forecasting of NE Monsoon rainfall (Oct-Dec) using indigenously developed statistical models based on principal component analysis (PCA). The parameters used for the statistical models are shown in Fig. 6.17. Overall, five predictors are used for long range prediction of NE monsoon rainfall. Out of these five predictors, four predictors are

derived from the Indian and West Pacific regions, while the fifth parameter is derived from the Atlantic Ocean. Since the inter-annual variability of NE monsoon rainfall is quite large (25%), developing a skillful statistical prediction scheme could be challenging. IMD, however, shares the long-range forecasts confidentially with the concerned state governments every year. Therefore, more research studies are required to understand the inter-annual variability of NE monsoon rainfall better and develop skillful long-range forecast models.

Rajeevan et al. (2012) suggested that present-day dynamical models have serious problems in properly simulating mean monsoon rainfall and its teleconnections. Coupled climate models do not correctly simulate the sign of the ENSO-NE Monsoon rainfall relationship. Furthermore, there is absolutely no skill with the present dynamical models in predicting inter-annual variability of NE monsoon.

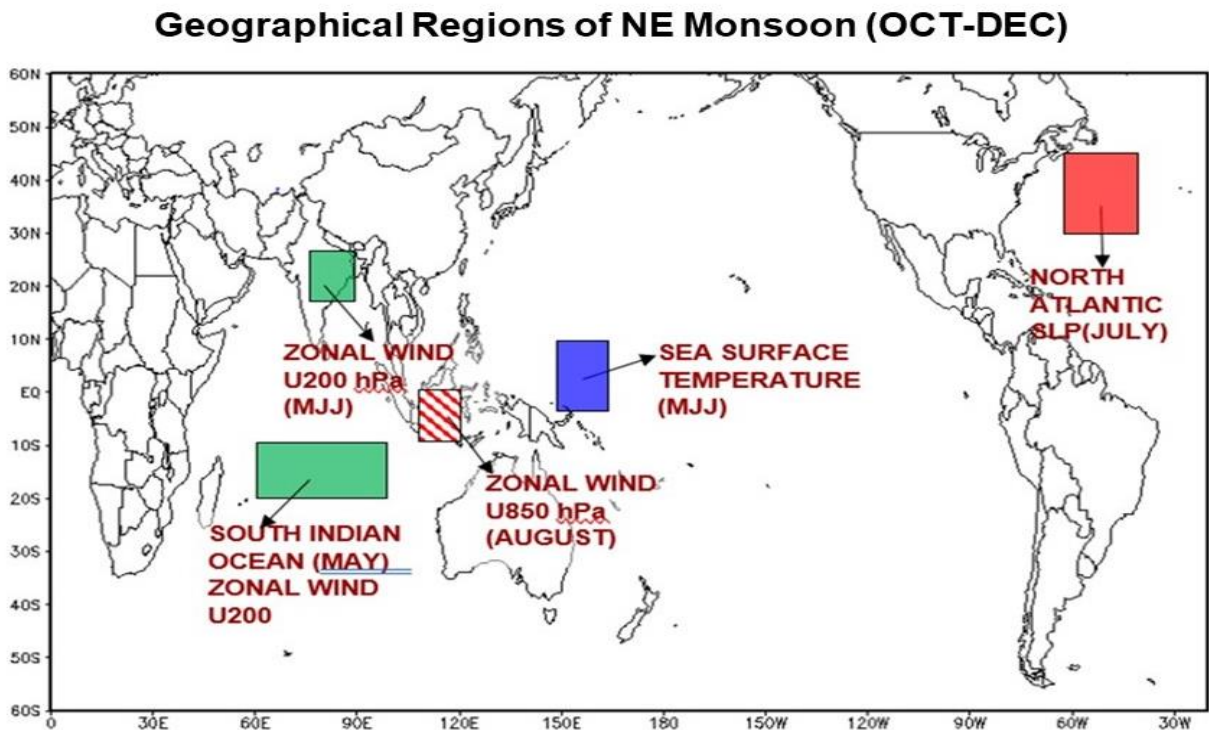


Fig. 6.17. The parameters used in the statistical model for the long-range forecasting of NE Monsoon rainfall by the India Meteorological Department.

The study by Acharya et al. (2011) suggested that the general circulation models considered in the study are not able to simulate the observed interannual variability of rainfall. They attributed this to inaccurate response of the models to sea surface temperatures. They found that the multi-model ensemble scheme improved the accuracy of simulations. The study by Sengupta and Nigam (2019) revealed that the historical twentieth-century climate simulations informing the Intergovernmental Panel on Climate Change's Fifth Assessment (IPCC-AR5) showed varied deficiencies in the NEM rainfall distribution and a markedly weaker (and often unrealistic) ENSO–NEM rainfall relationship.

Prasanna et al. (2021) examined the fidelity of the eight Asia-Pacific Economic Cooperation (APEC) Climate Center (APCC) models in representing the inter-annual variability and decadal shift in the northeast monsoon (NEM; October–December) rainfall over Southern Peninsular India (SPI). The observations showed a clear inter-annual and inter-decadal variability of NE monsoon rainfall. The analysis suggested that most of the models exhibited poor skill in representing the inter-annual variability. Only APCC model rainfall is in phase with observed SPI rainfall variations on the inter-annual time scale. More research work is required to improve both the statistical and dynamical models in making reliable long-range forecasts of NE Monsoon rainfall in the coming years.